MINISTÉRIO DA EDUCAÇÃO
UNIVERSIDADE FEDERAL DE ALFENAS – UNIFAL MG
PROGRAMA DE PÓS-GRADUAÇÃO EM
BIOCIÊNCIAS APLICADAS À SAÚDE

CAROLINA GIROTTO PRESSETE

PIPERINE-CHLOROGENIC ACID HYBRIDS MODULATE CRITICAL REGULATORS OF THE CELL CYCLE AND INHIBIT THE PROLIFERATION OF MELANOMA CELLS

Alfenas - MG
Setembro/2022

CAROLINA GIROTTO PRESSETE

PIPERINE-CHLOROGENIC ACID HYBRIDS MODULATE CRITICAL REGULATORS OF THE CELL CYCLE AND INHIBIT THE PROLIFERATION OF MELANOMA CELLS

Tese apresentada como parte dos requisitos para obtenção do título de Doutor em Biociências Aplicadas à Saúde.
Área de Concentração: Fisiopatologia
Orientadora: Profa. Dra. Marisa Ionta
Colaborador: Prof. Dr. Claudio Viegas Junior

Alfenas - MG
Setembro/2022

Sistema de Bibliotecas da Universidade Federal de Alfenas
Biblioteca Central

Pressete, Carolina Girotto.
Piperine-chlorogenic acid hybrids modulate critical regulators of the cell cycle and inhibit the proliferation of melanoma cells / Carolina Girotto Pressete. - Alfenas, MG, 2022.
63 f. : il. -

Orientador(a): Marisa Ionta.
Tese (Doutorado em Biociências Aplicadas à Saúde) - Universidade Federal de Alfenas, Alfenas, MG, 2022.
Bibliografia.

1. N-hydrazone subunit. 2. Molecular hybridization. 3. Melanoma cells. 4. Cell cycle arrest. 5. Apoptosis. I. Ionta, Marisa, orient. II. Título.

Ficha gerada automaticamente com dados fornecidos pelo autor.

Carolina Girotto Pressete

Piperine-chlorogenic acid hybrids modulate critical regulators of the cell cycle and inhibit the proliferation of melanoma cells

A Banca examinadora abaixo-assinada aprova a Tese apresentada como parte dos requisitos para a obtenção do titulo de Doutora Ciências pela Universidade Federalde Alfenas. Área de concentração: Biociências aplicadas à Saúde.

Aprovada em: 26 de agosto de 2022

Prof. Dr. Profa. Dra. Marisa Ionta

Instituição: Universidade Federal de Alfenas
UNIFAL-MG

Profa. Dra. Graziela Domingues de Almeida Lima
Instituição: Universidade Federal de Alfenas
UNIFAL-MG

Profa. Dra. Lusânia Maria Greggi Antunes
Instituição: Universidade de São Paulo
USP

Profa. Dra. Pollyanna Francielli de Oliveira
Instituição: Universidade Federal de Alfenas
UNIFAL-MG

Profa. Dra. Marta Miyazawa

Instituição: Universidade Federal de São Paulo
UNIFESP

Documento assinado eletronicamente por **Marisa Ionta**, **Professor do Magistério Superior**, em 26/08/2022, às 12:04, conforme horário oficial de Brasília, com fundamento no art. 6º, § 1º, do Decreto nº 8.539, de 8 de outubro de 2015.

Documento assinado eletronicamente por **Pollyanna Francielli de Oliveira**, **Professor do Magistério Superior**, em 26/08/2022, às 13:10, conforme horário oficial de Brasília, com fundamento no art. 6º, § 1º, do Decreto nº 8.539, de 8 de outubro de 2015.

Documento assinado eletronicamente por **Graziela Domingues de Almeida Lima**, **Professor(a) Visitante**, em 26/08/2022, às 13:47, conforme horário oficial de Brasília, com fundamento no art. 6º, § 1º, do Decreto nº 8.539, de 8 de outubro de 2015.

Documento assinado eletronicamente por **Marta Miyazawa**, **Usuário Externo**, em 26/08/2022, às 15:09, conforme horário oficial de Brasília, com fundamento no art. 6º, § 1º, do Decreto nº 8.539, de 8 de outubro de 2015.

Documento assinado eletronicamente por **Lusânia Maria Greggi Antunes**, **Usuário Externo**, em 31/08/2022, às 15:43, conforme horário oficial de Brasília, com fundamento no art. 6º, § 1º, do Decreto nº 8.539, de 8 de outubro de 2015.

A autenticidade deste documento pode ser conferida no site https://sei.unifal-mg.edu.br/sei/controlador_externo.php?acao=documento_conferir&id_orgao_acesso_externo=0, informando o código verificador **0797472** e o código CRC **7DA7B62D**.

AGRADECIMENTOS

Gostaria de agradecer à Deus por todas as oportunidades que me proporciona.

Aos meus pais, em especial minha mãe, por todo o apoio durante essa jornada. Vocês se sacrificaram e se dedicaram para que eu pudesse ter essa oportunidade e uma boa formação profissional.

À minha orientadora, Professora Dra. Marisa Ionta, por toda a orientação nesses anos do doutorado e sempre foi um exemplo como profissional.

À profa. Dra. Ester Caixeta e ao prof. Dr. Claudio Viegas Junior pela colaboração e participação ativa ao longo do desenvolvimento do projeto.

Aos amigos do LABAInt e LAPAN e professores do Departamento de Biologia Celular e do Desenvolvimento (DBCD), em especial, ao Dr. Guilherme Álvaro Ferreira da Silva pelos ensinamentos e convivência ao longo do tempo em que passei no Departamento.

Ao prof. Dr. Valdemar Antônio Paffato Junior, ex-coordenador do PPGB, pela dedicação ao Programa e pela atenção dispensada a mim em vários momentos dessa jornada acadêmica.

À Adriana, secretaria do PPGB, pela dedicação e constante apoio aos alunos do Programa.

À UNIFAL-MG, onde permaneci por dez anos da minha vida, pela oferta de excelentes oportunidades.

Ao CNPq, CAPES e FAPEMIG, pelo apoio financeiro. O presente trabalho foi realizado com apoio da Coordenação de Aperfeiçoamento de Pessoal de Nível Superior -Brasil (CAPES) - Código de Financiamento 001.

RESUMO

O melanoma é considerado a forma mais agressiva de câncer de pele devido ao seu alto potencial metastático. Apesar da introdução de novas abordagens terapêuticas, como imunoterapia e terapias direcionadas, a taxa de mortalidade permanece alta. A resistência tumoral (intrínseca e adquirida) representa um desafio para o tratamento do melanoma independentemente do esquema de tratamento adotado. Nesse cenário, é importante identificar novos candidatos a fármacos para melhorar as propostas terapêuticas para o melanoma. É importante ressaltar que os produtos naturais têm sido usados como protótipos para o desenvolvimento de novos candidatos à fármacos antineoplásicos. No presente estudo, foi investigado o potencial antitumoral de uma série de híbridos piperina-ácido clorogênico. As substâncias sintetizadas foram obtidas por hibridização molecular envolvendo os grupos farmacofóricos da piperina (1) e do ácido clorogênico (2), os quais foram unidos por um espaçador *N*-acilhidrazona (3). Os compostos foram testados frente as linhagens celulares derivadas de melanoma (SK-MEL-147, WM-1366, CHL-1), as quais são representativas de diferentes subtipos de melanoma. O ensaio de viabilidade celular revelou que a linhagem SK-MEL-147 foi mais responsiva aos tratamentos em relação às linhagens WM-1366 e CHL-1. Com base nos valores de IC_{50}, as substâncias PQM-277, PQM 281 e PQM 286 foram as mais ativas da série. Estudos adicionais mostraram que PQM-277 induz bloqueio do ciclo celular na transição G2/M, enquanto os compostos PQM 281 e PQM 286 inibem a progressão do ciclo na transição G1/S. Os resultados referentes a investigação dos mecanismos moleculares associados à atividade antiproliferativa dessas substâncias sobre a linhagem SK-MEL-147 mostraram que PQM-277 foi capaz de modular a expressão de reguladores críticos da transição G2/M e progressão pelas fases iniciais da mitose. Houve redução da abundância de mRNA para *CCNB1* (ciclina B1), *CDK1, AURKA* (Aurora A), *AURKB* (Aurora B) e *PLK1*. Por outro lado, os níveis de expressão de mRNA de *CDKN1A* (p21), um regulador negativo do ciclo celular, aumentaram nas amostras tratadas com PQM-277 quando comparados aos grupos controle. Com relação à atividade antiproliferativa de PQM 281 e 286, nós demonstramos que essas substâncias inibem a progressão do ciclo celular por reduzir os níveis de expressão das ciclinas D e E. Além disso, nós evidenciados que as substâncias PQM 277, PQM 281 e PQM 286 tem atividade pró-apoptótica frente a linhagem SK-MEL-147. Houve aumento dos níveis de expressão de *BAX* com concomitante redução na abundância de RNA mensageiro para *Bcl-2* em amostras tratadas com PQM 277, indicando que houve ativação da apoptose pela via intrínseca. Tomados em conjunto, os dados obtidos no presente estudo demonstram que os híbridos de piperina e ácido clorogênico são promissores protótipos antitumorais e devem ser considerados em futuras investigações envolvendo modelos animais.

Palavras-chave: subunidade *N*-hidrazona, hibridização molecular, células de melanoma, parada do ciclo celular, apoptose.

ABSTRACT

Melanoma is considered the most aggressive form of skin cancer due to its high metastatic potential. Despite the introduction of new therapeutic approaches such as immunotherapy and target-directed therapies, the mortality rate remains high. Intrinsic and acquired tumor resistance represents a challenger for melanoma treatment independently of the treatment schedule adopted. In this scenario, it is important to identify new drug candidates to improve therapeutic proposals for melanoma. Importantly, natural products have been used as scaffolds for drug design and development of new anticancer prototypes. In the present study, the antitumor potential of a series of piperine-chlorogenic acid hybrids was investigated. The synthesized substances were obtained by molecular hybridization of the piperine (**1**) and chlorogenic acid (**2**) pharmacophore fragments using a *N*-acylhydrazone subunit as linker (**3**). The compounds were assayed against melanoma cell lines (SK-MEL-147, WM-1366, CHL-1), which are representative of different melanoma subtypes. Cell viability assay revealed that SK-MEL-147 was more responsive to treatments than WM-1366 and CHL-1 cell lines. Based on IC_{50} values, PQM-277, PQM 281, and PQM 286 were the most active compounds. Further investigations showed that PQM-277 induces cell cycle arrest at G2/M, while the compounds PQM 281 and PQM 286 inhibit cell cycle progression at G1/S. The molecular mechanism associated with the antiproliferative activity of these substances on SK-MEL-147 was investigated. The data showed that PQM-277 modulates the expression of critical regulators for G2/M transition and mitosis onset. There was a reduction of mRNA abundance for *CCNB1* (cyclin B1), *CDK1*, *AURKA* (Aurora A), *AURKB* (Aurora B), and *PLK1*. Conversely, the mRNA expression levels of *CDKN1A* (p21), a negative regulator of the cell cycle, were upregulated in samples treated with PQM-277 when compared to control groups. Concerning antiproliferative activity of PQM 281 and 286, we demonstrated that these substances inhibit cell cycle progression by inducing cyclins D and E downregulation. In addition, the pro-apoptotic activity of the compounds PQM-277, PQM-281, and PQM-286 on SK-MEL-147 cells was evidenced. There was a concomitant *BAX* upregulation and *Bcl-2* downregulation in samples treated with PQM-277, that in turn, contributed to intrinsic apoptosis pathway activation. Taken together, the data obtained in this study demonstrate that piperine-chlorogenic acid hybrids are promising pre-clinic prototypes and should be considered for further *in vivo* investigation.

Keywords: *N*-hydrazone subunit, molecular hybridization, melanoma cells, cell cycle arrest, apoptosis.

SUMMARY

1 INTROUCTION

Cancer is a multifactorial disease including interactions of complex genetic/epigenetic and environmental factors. Cancer cells exhibit some features that include uncontrolled proliferation and high invasiveness ability (CHAFFER; WEINBERG, 2011; HANAHAN; WEINBERG, 2011; HANAHAN; WEINBERG; FRANCISCO, 2000). Melanoma is an aggressive malignant tumor related to 75% of deaths by skin cancer. Overall, melanomas have more mutations than any other cancer type, and its lethality is associated to its high capacity to form metastases (GROSSMAN *et al*., 2020; SCHADENDORF *et al*., 2015).

The main risk factor for melanoma includes UV exposure, which lead to genetic alterations resulting in a high mutation rate *(EGGERMONT et al., 2014; SCHADENDORF et al*., 2015). According to epidemiological data, the incidence and mortality rates for melanoma have been increasing in recent years and the available therapeutic proposals are few effective. Intrinsic or acquired resistance of the tumor cells to drug available represent an important obstacle to be overcome (EGGERMONT *et al*., 2014; GROSSMAN *et al*., 2020; SIEGEL; MILLER, 2019; SIEGEL; MILLER; JEMAL, 2016). Hyperactivation in MAPK (mitogen-activated protein kinase) RAF/MEK/ERK signaling pathway is commonly observed in melanomas due to *NRAS* or *BRAF* activating mutations (CURTIN *et al*., 2005; HELD, 2010). Moreover, mutation in *NF1*, *TERT*, *CDKN2A, TP53* and *PTEN* also are observed in melanomas (SHAIN; BASTIAN, 2016).

Therapeutic approaches for melanoma comprise surgical removal, radiotherapy and systemic therapies. Based on melanoma features, the systemic treatment may include cytotoxic drugs, immunomodulators and/or BRAF and MEK inhibitors (SCHADENDORF *et al*., 2015; GROSSMAN *et al*., 2020). Even though advances in melanoma treatment in the last decade, the mortality rate remains high. Intrinsic and acquired resistance are frequently associated to tumor progression and metastasis. In this way, it is imperative to identify new drug prototypes with antitumor activity.

The natural compounds are known sources of bioactive compounds with pharmacological potential. It has been reported that piperine (**1**) and chlorogenic acid (CGA) (**2**) (Figure 1) display a spectrum of pharmacological proprieties including antitumor activity (CHEN *et al*., 2020; DING *et al*., 2018; GORGANI *et al*., 2017). (**1**) has been preferentially isolated from black pepper (*Piper nigrum L.*) and long pepper (*Piper longum L.*) (CHEN *et al*.,

2020; DING *et al*., 2018; GEORGE; SUSAN; MALATHI, 2019), while (**2**) is found in plants, fruits and vegetables (BAGDAS *et al*., 2014; BAGDAS; CINKILIC; YUCEL, 2012). Considering the antitumor potential of the (**1**) and (**2**) and the continuous search for new substances that can improve therapeutic proposals for metastatic melanoma, we explored their chemical scaffolds to obtain a series of hybrid compounds, which antitumor potential was investigated. Through of molecular hybridization technique the benzo[d]1,3-dioxole moiety from piperine (**a**) and cinnamoyl fragment (**b**) from CGA were connected by acylhydrazone spacer subunit (**c**) (Figure 1). The introduction of acylhydrazone linker can contribute to improve physico-chemical and pharmacological properties of synthesized substances (LIMA; BARREIRO, 2005). The piperine-chlorogenic acid hybrids were synthesized in collaboration with Dr. Claudio Viegas Junior from Chemistry Institute/UNIFAL-MG.

Figure 1- Design of a new series of piperine-chlorogenic acid acylhydrazone hybrid derivatives.

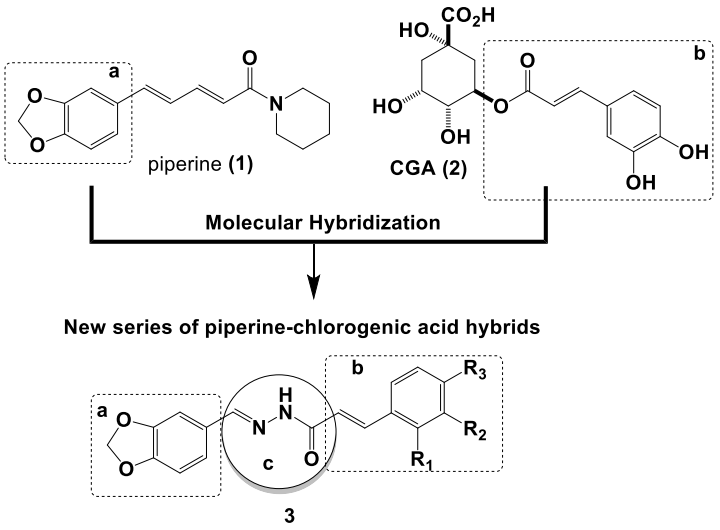

Source: From the author

Note: Piperine-chlorogenic acid acylhydrazone hybrid derivatives (**3**) by molecular hybridization of structural fragments from piperine (**1**) and chlorogenic acid (**2**, CGA) connected by an acylhydrazone subunit.

2 LITERATURE REVIEW

2.1 CANCER AND MELANOMA

Cancer is recognized as a group of diseases characterized by uncontrolled cell growth and the spread of abnormal cells, which can invade and colonize healthy tissues (CHAFFER; WEINBERG, 2011; HANAHAN; WEINBERG, 2011; HANAHAN; WEINBERG; FRANCISCO, 2000). This disease is considered a major public health problem worldwide and an important barrier to increasing life expectancy in every country of the world, furthermore, represents the second leading cause of death in the world (SIEGEL; MILLER, 2019, 2020; SIEGEL; MILLER; JEMAL, 2016; SUNG *et al*., 2021). Cancer incidence and mortality are growing rapidly worldwide. The reasons are complex, but reflect population aging and growth, as well as changes in the prevalence and distribution of major cancer risk factors, several of which are associated with socioeconomic development (BRAY; FERLAY; SOERJOMATARAM, 2018; SUNG *et al*., 2021).

In 2018, worldwide, there were an estimated 18.1 million new cases of cancer and 9.6 million deaths (BRAY; FERLAY; SOERJOMATARAM, 2018). In 2020, there were an estimated 19.3 million new cases and 10 million cancer deaths worldwide. Europe was accounts for 22.8% of the total cancer cases and 19.6% of the cancer deaths, followed by the Americas' 20.9% of incidence and 14.2% of mortality worldwide (SUNG *et al*., 2021). The most frequently diagnosed cancers in 2020 to men are prostate (21%), lung (13%) and colorectal (9%) cancers, while in women the most frequent are breast cancers (30%), lung (12%) and colorectal (8%) (BRAY; FERLAY; SOERJOMATARAM, 2018; SIEGEL; MILLER, 2020). Although, in 2021 the most frequently diagnosed cancers in men are prostate (26%), lung (12%), and colorectal (8%) cancers, while in women the most frequent are breast cancers (30%), lung (13%) and colorectal (8%) (SIEGEL; MILLER, 2021).

Despite efforts to introduce new therapeutic approaches, cancer remains a major concern worldwide, as it is the second leading cause of death and is preceded only by cardiovascular diseases (SIEGEL; MILLER, 2019, 2020; SIEGEL; MILLER; JEMAL, 2016). Although traditional therapies such as surgery, chemotherapy and radiotherapy have effects in the treatment of the disease, some patients are refractory to treatment or become resistant to available therapeutic proposals (ASATI; MAHAPATRA; BHARTI, 2016; DRÃGÃNESCU; CARMOCAN, 2017; RIBEIRO *et al*., 2016). Consequently, there is an urgent need to identify

new agents that can improve therapeutic proposals. In this context, substances capable of inhibiting the proliferative and invasive behavior of tumor cells, as well as reducing resistance to signals of death may be useful for the development of new anticancer drugs (ASATI; MAHAPATRA; BHARTI, 2016; PETERSON *et al*., 2010).

Melanoma is considered the most aggressive form of skin cancer and, although the incidence rate is low compared to other types of cancer, it is a highly lethal type of cancer and represents one of the main causes of death from skin diseases (FOFARIA; KIM; SRIVASTAVA, 2014). Melanoma is also responsible for 80% of skin cancer-related deaths due to its high metastatic potential (MILLET; MARTIN; RONCO, 2017). According to the American Cancer Society, there were an estimated 96,480 cases of melanoma in the United States and 7,230 deaths from the disease in 2018 (SIEGEL; MILLER, 2019). In Brazil, although skin cancer is the most frequent and corresponds to about 30% of all malignant tumors registered in the country, melanoma represents only 3% of malignant skin neoplasms (BRASIL, 2020). Estimates made by the National Cancer Institute (INCA) for the year 2020 show that there will be 8,450 new cases of melanoma in Brazil, with 4,200 cases in men and 4,250 in women.

Melanoma originates from a series of genetic and epigenetic alterations that favor the process of tumor invasion and progression (GUARNERI *et al*., 2017). Melanoma mainly affects the Caucasian population of both sexes and has a very poor prognosis when it is diagnosed at an advanced stage (JIANG *et al*., 2017; RAHMATI *et al*., 2020). Moreover, Tumor thickness is the most important prognostic factor in primary melanoma. Therefore, early identification of melanoma is crucial for successful treatment (LEITER; GARBE, 2008). Melanoma can be categorized into cutaneous (approximately 90% of melanoma cases) and non-cutaneous (CURTIN *et al.*, 2005; EDDY; CHEN, 2020; ISOLA; EDDY; CHEN, 2016). Non-cutaneous melanoma has a worse prognosis than cutaneous melanoma, due to the delay in primary tumor diagnosis, the aggressive nature of these tumors, a high recurrence rate after treatment, and a poor overall survival (EDDY; CHEN, 2020; KUK *et al*., 2016). Epidemiology studies provided strong evidence that fair skinned individuals have a higher susceptibility to cutaneous melanoma, while darker skinned individuals have higher cases of non-cutaneous melanoma (EDDY; CHEN, 2020; WU *et al*., 2006).

Studies show that excessive exposure to sunlight represents a critical factor for the development of melanoma, especially in Caucasians (EGGERMONT *et al*., 2014; RAHMATI *et al*., 2020; SHAIN; BASTIAN, 2016). Ultraviolet radiation (UVR) is the main environmental

risk factor for the development of melanoma and are estimated to be responsible for the appearance of approximately 65% of all melanomas, thus effective protection from the sun is an important preventive measure (EMRI; JANKA; JANKA, 2018; GUARNERI *et al*., 2017; LEONARDI *et al*., 2018; RAHMATI *et al*., 2020; SHAIN; BASTIAN, 2016). Artificial sources of UV light must also be considered and has been also linked to an increased risk of developing melanoma (EMRI; JANKA; JANKA, 2018; LEONARDI *et al*., 2018). The polymorphisms of the melanocortin 1 receptor (MC1R) gene, are responsible for the different human skin-color phenotypes, thus, individuals with characteristics, such as red hair, a light complexion and light eyes exhibit a low pigmentation, with a consequent heightened sensitivity to UV exposure (DESSINIOTI *et al*., 2011; LEONARDI *et al*., 2018). Individuals with high number of melanocytic nevi have increased risk of melanoma, although increased number of nevi are also linked in part to excessive early life sun exposure (EMRI; JANKA; JANKA, 2018; LEONARDI *et al*., 2018). However, the number of congenital and acquired melanocytic nevi, genetic susceptibility and family history are factors associated with the development of the disease (HAWKES; TRUONG; LAURENCE, 2016; LEONARDI *et al*., 2018). Thus, melanoma is considered a heterogeneous disease that involves different tumor subtypes, which present different behaviors and clinical characteristics depending on the factors associated with their development (EMRI; JANKA; JANKA, 2018).

The development of melanoma involves different stages and, in general, five stages are observed considering the histological characteristics: 1) nevus, a benign lesion characterized by the quantitative increase of melanocytes; 2) dysplastic nevus, characterized by an atypical organization of cells; 3) melanoma in the radial growth phase, a stage in which melanocytes proliferate intensely in the epidermis; 4) melanoma in the vertical growth phase, a stage in which the cells penetrate the basal lamina and invade the dermis and subcutaneous tissue; 5) metastatic melanoma, characterized by the spread of cells in the skin and other organs (CLARK, 1991; HERLYN, 1990; RAHMATI *et al*., 2020; SHAIN; BASTIAN, 2016).

In the last decades, many studies have been carried out aiming to collect information related to the genomic changes associated with melanoma development and progression. The understanding of the molecular mechanisms related to the transformation process was very important for the development of new therapeutic protocols for patients diagnosed with melanoma. Immunotherapy and target-directed therapies were introduced as alternatives to cytotoxic therapy and represent promising therapeutic approaches for melanoma, however there was a small increase in the survival rate, in general, due to the development of resistance to

available drugs. However, the prognosis of this type of cancer can be considered good if detected in its early stages (EMRI; JANKA; JANKA, 2018; HODI *et al*., 2010; SINGH; SALAMA, 2016).

Over the past years, a deeper understanding of melanoma development and biology has been reached. Studies show that melanoma is associated with a series of somatic mutations in genes that regulate cell proliferation, survival and death *(AKBANI et al., 2015; LEONARDI et al*., 2018). In most melanomas, somatic mutations affect genes that control important cellular processes, such as proliferation (*BRAF, NRAS* and *NF1*), growth and metabolism [phosphatase and tensin homolog (*PTEN*)], resistance to apoptosis [tumor protein p53 (TP53)], cell cycle control [cyclin-dependent kinase inhibitor 2A (*CDKN2A*)]. These genomic alterations typically lead to the aberrant activation of two main signaling pathways in melanoma: The RAS/RAF/MEK/ERK signaling cascade [also known as the mitogen-activated protein kinase (MAPK) pathway] and the phosphoinositol-3-kinase (PI3K)/AKT pathway. (CHAPPELL *et al*., 2011; HODIS *et al*., 2012; LEONARDI *et al*., 2018; RAHMATI *et al*., 2020; SCHADENDORF *et al*., 2015).

The RAF/MEK/ERK MAPK (*mitogen-activated protein kinase*) is constitutively activated in melanoma due to activating mutations in proto-oncogenes *NRAS* (15-30%), *NF1* (10-15%) or *BRAF* (50-70%) (CARLINO *et al*., 2015; CURTIN *et al*., 2005; HELD, 2010; LEONARDI *et al*., 2018; RAHMATI *et al*., 2020; SHAIN; BASTIAN, 2016). The MAPK pathway is physiologically involved in the transduction of extracellular signals, such as growth factors and hormones leading to the expression of genes that are central drivers of cell proliferation, differentiation, migration and survival (CURTIN *et al*., 2005; HODIS *et al*., 2012; LEONARDI *et al*., 2018; MADAK-ERDOGAN *et al*., 2011; ZHANG *et al.*, 2016). Mutations in *BRAF* and *NRAS* are associated with a worse prognosis (JAKOB *et al*., 2012). Missense BRAF mutation is frequently observed in melanoma. The mutation that determine amino acid substitution of valine to glutamic acid (V600E) occurs up to 80-90% of cases (LEONARDI *et al.*, 2018; RAHMATI *et al*., 2020; RUBINSTEIN *et al*., 2010; SCHADENDORF *et al*., 2015; SHAIN; BASTIAN, 2016).

Mutations in *NRAS* and *PTEN* in melanoma most commonly involve activation of the PI3K/AKT pathway. Somatic mutations in *PTEN* are observed in 14% of cases (PAPPALARDO *et al*., 2016; ZHANG *et al*., 2016). The PI3K pathway is normally involved in cellular homeostasis and its activation has been demonstrated to be central in different cancer

types, including melanoma where it is the second most frequently activated pathway (DAVIES, 2012; LEONARDI *et al*., 2018; RAHMATI *et al*., 2020).

NF1 is a tumor suppressor gene that encodes NF1 protein, which regulates the RAS family by converting the active RAS-guanosine triphosphate (RAS-GTP) to the inactive RAS-guanosine diphosphate (RAS-GDP), thereby inhibiting downstream RAS signaling. Therefore, *NF1* loss-of-function determines the hyperactivation of NRAS protein and thus, increased MAPK and PI3K pathways signaling (KRAUTHAMMER *et al*., 2015; MAERTENS *et al*., 2013; NISSAN *et al*., 2014; RAHMATI *et al*., 2020).

CDKN2A and *CDKN1A* genes encode negative regulators of the cell cycle. The *CDKN2A* encodes two proteins by alternative *splicing* $p14^{ARF}$ and $p16^{INK4A}$ that inhibit MDM2 and CDK4/6, respectively. While, *CDKN1A* encodes p21 protein, which acts as a universal inhibitor of CDKs (LEONARDI *et al*., 2018; RAHMATI *et al*., 2020; SCHADENDORF *et al*., 2015; SHAIN *et al*., 2015). *(LEONARDI et al., 2018; RAHMATI et al.*, 2020; SCHADENDORF *et al*., 2015; SHAIN *et al.*, 2015).

TP53 mutations are found in approximately 20% of metastatic melanomas. However, mutational studies indicate that TP53 mutations may arise later during melanoma development. The *TP53* mutation rate was lower in primary melanoma compared to samples derived from metastases sites (HODIS *et al*., 2012; KRAUTHAMMER *et al*., 2015; SHAIN; BASTIAN, 2016). Furthermore, mutations in the *TP53* gene can result in loss of p53 tumor suppressor function or acquisition of oncogenic functions and therefore are critical in the process of tumor progression (SCHADENDORF *et al.*, 2015; SHAIN; BASTIAN, 2016).

In the last decade, several drugs have been approved by the *Food and Drug Administration* (FDA) for the treatment of metastatic melanoma including inhibitors of BRAF (vemurafenib, dabrafenib, and encorafenib) and MEK ((trametinib, cobimetinib, and binimetinib) for tumor that display hyperactivation of RAF-MEK-ERK (MAPK) signaling pathway (ASCIERTO *et al*., 2016; DUMMER *et al.*, 2018; EGGERMONT *et al.*, 2014; ROBERT *et al*., 2019). Notably, immunomudulators also have been approved for melanoma treatment, such as vemurafenib (DOBRY *et al*., 2018).

Studies show that the combination of BRAF and MEK inhibitors has been more effective compared to the isolated use of BRAF inhibitors *(DUMMER et al., 2018; HODI et al.*, 2016; LONG *et al.*, 2014; OLBRYT *et al.*, 2020; ROBERT *et al*., 2019). Thus, the combination of these agents has been recommended as a first-line therapy for patients with

melanoma who carry the BRAF V600 mutation, which is present in up to 60% of cases (ROBERT *et al.*, 2019).

With the introduction of new therapeutic approaches, the one-year relative survival rate for metastatic melanoma has increased from 42% for patients diagnosed between 2008 and 2010 to 55% for those diagnosed between 2013 and 2015 (SIEGEL; MILLER, 2020). (SIEGEL; MILLER, 2020). Despite the advances observed with the introduction of alternative therapies, melanoma mortality rate remains high. In general, the tumor progression occurs due to development of resistance to available drugs. Thus, it is imperative to search for both new therapeutic targets and innovative drug candidates.

2.2 CHLOROGENIC ACID AND PIPERINE

Natural products represent important sources for the identification of new substances with pharmacological properties (NEWMAN; CRAGG, 2016). Importantly, many natural compounds have been used as chemical scaffolds in drug design including phenolic compounds. Studies show that phenolic compounds act as therapeutic or preventive agents against different pathological conditions including cancer, inflammatory and cardiovascular diseases, and neurodegenerative diseases (SCALBERT *et al*., 2007) .

Chlorogenic acid (5-caffeoylquinic acid, CGA), formed by the esterification of caffeic and quinic acids, is a natural phenolic compound present in plants, fruits and vegetables (BAGDAS *et al*., 2014; BAGDAS; CINKILIC; YUCEL, 2012), such as sweet potatoes (FILHO *et al*., 2019), green tea and coffee beans (BAGDAS *et al*., 2014), apples (SUT *et al.*, 2019), among others. Studies show that chlorogenic acid has antioxidant, anti-inflammatory, analgesic and antitumor properties (BAGDAS *et al*., 2014; BAGDAS; CINKILIC; YUCEL, 2012; CINKILIC *et al*., 2013; HUANG *et al*., 2019; SATO *et al*., 2011; SUT *et al.*, 2019; WENG; YEN, 2012). CGA has also been reported to have antagonistic and free radical scavenging effects against lipid peroxidation in different organs (OBOH; AGUNLOYE; ADEFEGHA, 2013).

According to Refolo *et al*. (2018), CGA potentiates the antiproliferative and pro-apoptotic activity of regorafenib, a tyrosine kinase inhibitor, by activating Bax and Caspase 3/7, and by inhibiting Bcl2 and Bcl-xL on cells derived from hepatoma (HepG2). Antiproliferative activity of the CGA on colon cancer carcinoma cells (Caco-2) has been reported (EKBATAN *et al.*, 2018). In addition, CGA was able to inhibit proliferation and induce apoptosis of

osteosarcoma by modulating extracellular signal-regulated kinase1/2 (ERK1/2) activation (SAPIO *et al*., 2019). Pro-apoptotic activity of CGA was associated to its ability to increase Bax/Bcl-2 ratio and inhibit PI3K/Akt/mTOR signaling pathway in kidney-derived cells (WANG *et al.*, 2019). Therefore, CGA display antitumor potential by acting on different molecular target and inhibit oncogenic pathways (BONESI *et al*., 2018; CHANG; CHANG; TSENG, 2018; REFOLO *et al*., 2018; WANG *et al*., 2019; LIU *et al.*, 2019).

Piperine (1-peperoylpiperidine) is an alkaloid found in plants, which has been isolated mainly from black pepper (Piper nigrum L.) and long pepper (Piper longum L.) (CHEN *et al*., 2020; DING *et al.*, 2018; GEORGE; SUSAN; MALATHI, 2019). Piperine exhibits a variety of pharmacological properties, acting as an antioxidant (SELVENDIRAN; BANU; SAKTHISEKARAN, 2004), anti-inflammatory (YING *et al*., 2013), anti-angiogenic (DOUCETTE *et al*., 2013), neuroprotective, antibacterial agent. , hepatoprotective (GORGANI *et al.*, 2017). Antiproliferative activity of the piperine has been demonstrated against a variety of tumor cells (CHEN *et al*., 2020; GEORGE; SUSAN; MALATHI, 2019; GUO *et al*., 2019; OUYANG *et al*., 2013; SAMYKUTTY *et al*., 2013; SI *et al*., 2018).

Study carried out by Lai *et al*. (2012) showed that the piperine inhibits the growth in mouse breast cancer cells (4T1) and induces apoptosis of these cells. The authors demonstrated that piperine treatment induced caspase 3 activation and reduced cyclin B1 expression levels. Two other studies show that piperine treatment resulted in a dose-dependent inhibition of the proliferation of androgen-sensitive (LNCaP) and insensitive (PC-3) prostate cancers, causing cell cycle arrest at G0/G1 and reducing the expression of cyclin D1 and cyclin A (GEORGE; SUSAN; MALATHI, 2019; OUYANG *et al.*, 2013). In addition, Samykutty *et al*. (2013) showed that piperine-treated prostate cancer strains (LNCaP and PC-3) resulted in reduced expression of phosphorylated STAT-3 and nuclear factor-kB (NF-kB) transcription factors, which has already been shown to play a role in angiogenesis and in the invasion of prostate cancer cells. In triple negative breast cancer (TNBC) (MDA-MB-231) and ER/PR positive breast cancer (MCF-7) lines, piperine treatment reduced phosphorylated STAT-3 expression (CHEN *et al.*, 2020). Fofaria; Kim; Srivastava (2014) showed antiproliferative activity of the piperine on melanoma cells (SKMEL28 and B16F0), and demonstrated that inhibitory effects of the piperine on cell proliferation were due to its ability to induce cell cycle arrest at G1/S by modulation of cyclin D1 and p21 expression.

Based on findings, piperine display a potential as a therapeutic agent in the prevention and treatment of different types of cancer, however pharmacokinetic studies show that piperine

has low solubility and stability, aspects that restrict its clinical application (ZENG *et al*., 2017). Thus, it is necessary to obtain new chemical-structural standards that maintain the biological activity observed for piperine, but that gives to this substance a higher solubility coefficient.

3 OBJECTIVE

3.1 MAIN OBJECTIVE

Investigate the antitumor potential of a new series of piperine-Chlorogenic acid hybrids using melanoma cell lines as study model.

3.2 SPECIFIC OBJECTIVES

The objectives of the present work are to verify the capacity of PQM's in:

a) evaluate the influence of the synthesized substances on the proliferative behavior of melanoma-derived cell lines with different mutation profiles to select promising substances;
b) select lead substance based on the effects on cell cycle progression;
c) investigate molecular mechanism underlying antiproliferative activity of lead substance on melanoma cells;
d) evaluate whether the lead compound can modulate RAS/RAF/MEK/ERK and PI3K/AKT signaling pathways;
e) investigate the pro-apoptotic potential of the lead substance.

4 MATERIAL AND METHODS

4.1 HYBRIDS CHEMICAL STRUCTURES AND TREATMENT SCHEDULE

The piperine-chrorogenic acid derivatives were synthesized by Dr. Claudio Viegas Junior from Laboratory of Research on Medicinal Chemistry (Chemistry Institute, Federal University of Alfenas). Piperine and chlorogenic acid were used as prototype to obtain hybrids derivatives. The cynamoil and piperonyl pharmacophoric groups derived from chlorogenic acid and piperine, respectively, were linked by *N*-acylhidradone fragments. The series display different substituents on the aromatic ring derived from chlorogenic acid (Scheme 1).

Scheme 1- Synthetic route and global yields (GB) for the target-compounds **3a-i**

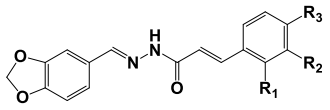

PQM-277 (**3a**): R_1= H; R_2= OCH_3; R_3= OH (GB: 49.5%)
PQM-279 (**3b**): R_1= OH; R_2= H R_3= H (GB: 58.6%)
PQM-280 (**3c**): R_1= H; R_2= H; R_3= OH (GB: 28.0 %)
PQM-281 (**3d**): R_1= H; R_2= H; R_3= H (GB: 35.6%)
PQM-284 (**3e**): R_1= H; R_2e R_3= methylenedioxy (GB: 15.5%)
PQM-285 (**3f**): R_1= H; R_2= H; R_3= CF_3 (GB: 70.7%)
PQM-286 (**3g**): R_1= OH; R_2= OCH_3; R_3=H (GB: 45.2%)
PQM-287 (**3h**): R_1= OCH_3; R_2= OCH_3; R_3= H (GB: 79.9%)
PQM-288 (**3i**): R_1= H; R_2= H; R_3=Cl (GB: 60.1%)

Source: From the author

Synthetic compounds were solubilized in dimethyl sulfoxide (DMSO), and stock solution (20 mM) was stored at -20º C until use. The substances were solubilized in fresh culture medium at final concentrations immediately before treatments. Cells were seeded into plates containing 96, 24, or 6 wells depending of the experimental approach. After attachment, the cells were treated for 24 or 48h.

4.2 CELL LINES AND CULTURE CELL CONDITIONS

Melanoma cell lines (SKMEL-147, CHL-1 e WM1366) and primary dermal fibroblast cell culture (FBM) (passages 2-10) were used in this study. Melanoma cell lines were purchased from Cell Bank of Rio de Janeiro and primary fibroblast were gently donated by Dr. Angel Mauricio Castro Gamero from Institute of Natural Science/ Federal University of Alfenas (Proc. 2.082.524). The cells were maintained in DMEM/F12 (Dulbecco's Modified Eagle's Medium

plus F12, Sigma, CA, USA) supplemented with 10% fetal bovine serum (Vitrocell, Campinas, Brazil). Cells were grown in a humidified atmosphere of 95% air and 5% CO2 at 37°C.

4.3 CELL VIABILITY ASSAY

Cell viability analysis was performed according to Vichai; Kirtikara (2006). The sulforhodamine B (SRB) assay was used for cell density determination, based on the measurement of cellular protein content. Melanoma cells were seeded into 96-well plates at a density of 1 x 10^4. After attachment, the cells were treated with different substances at 25 μM for 48 h. Cell monolayers were fixed with 10% trichloroacetic acid at 4ºC for 1h and stained with SRB (0.4%) for 30 min. Next, the samples were washed repeatedly with 1% acetic acid to remove unbound SRB. The protein-bound dye was dissolved in 10 mM Tris base solution for optical density (OD) determination at 540 nm with reference of 690, using a microplate reader.

4.4 CELL CYCLE ANALYSIS

Cell cycle analysis was performed according to Ferreira-Silva *et al*. (2017). Briefly, SK-MEL-147 cells were seeded into 35 mm Petri plates at a density of 1 x 10^5 cells/plate. Cell cultures were treated with PQM 277 at 5-10 μM, PQM 281 and PQM 286 at 10-20 μM for 24 h. Then, the samples were fixed with 75% ethanol at 4°C overnight, rinsed twice with cold phosphate-buffered saline (PBS). Afterwards, cells were homogenized in dye solution [PBS containing 90 μg.mL-1 propidium iodide (PI) and 1,5 mg. mL-1 RNAase]. The analysis was performed after 24 h using a flow cytometer (Guava easyCyte 8HT, Hayward, CA, USA). Results are presented as mean ± SD of three independent experiments.

4.5 CLONOGENIC ASSAY

Clonogenic assay was performed according to Franken *et al.* (2006). Briefly, 200 cells were seeded into 35 mm plates. Cells were treated PQM 277 at 5-10 μM, PQM 281 and PQM 286 at 10-20 μM μM for 24 h and recovered in a drug-free medium for subsequent 12 days. Afterwards, the colonies were fixed with methanol and stained with crystal violet. Only colonies with >50 cells were counted by direct visual inspection with a stereomicroscope at

20X magnification. Assays were performed in triplicate and data were presented as mean ± SD of three independent experiments.

4.6 MITOTIC INDEX DETERMINATION

Mitotic indexes were determined from fluorescent cytological preparations stained with DAPI and labeled for microtubule as previously described by Azevedo-Barbosa *et al*. (2019). Cells were seeded on coverslips in 35 mm Petri dishes at 1×10^5 cells/plate and treated with PQM 277 at 5 and 10 μM for 24 h and fixed with 3.7% formaldehyde for 30 min. Following membrane permeabilization step, anti-α-tubulin antibody (Sigma, T6199, 1:100) was incubated overnight. Secondary anti-mouse IgG-FITC antibody (1:100, Sigma Aldrich) was added to the sample and incubated for 2h. Nuclei were stained with fluoroshield with DAPI (Sigma Aldrich, F6057), and the coverslips were mounted on microscope slides. Analyses were performed using a fluorescence microscope (Nikon). Fluorescent cytological preparations were used to determine the frequency of mitosis (1,000 cells per sample were counted). The data are shown as the mean ± SD of three independent experiments.

4.7 P21 IMMUNODETECTION

Cells were seeded on coverslips in 35 mm Petri dishes at 1×10^5 cells/plate and treated with PQM 277 at 5 and 10 μM for 24. Cells were fixed with 3.7% formaldehyde for 30 min. Following membrane permeabilization step, p21 antibody (1:500, Cell signaling, #2947) was incubated overnight. Secondary anti-rabbit IgG-FITC antibody (1:100, Sigma Aldrich) was added to the sample and incubated for 2h. Nuclei were stained with fluoroshield with DAPI (Sigma Aldrich, F6057), and the coverslips were mounted on microscope slides. Analyses were performed using a fluorescence microscope (Nikon). Fluorescent cytological preparations were used to determine the frequency of p21 (500 cells per sample were counted). The data are shown as the mean ± SD of three independent experiments.

4.8 BrdU INCORPORATION ASSAY

Cells were seeded on coverslips in 35 mm Petri dishes at 1×10^5 cells/plate. Cell cultures were treated PQM 277 for 24 h at 5-10 μM. BrdU pulse (100 μM for 2 h) was performed at 37°C. After that, the cells were fixed in formaldehyde 3.7 % for 15 min and processed for immunofluorescence. For DNA denaturation 1.5 mol/L of HCl was used for 30 min. After washing, cells were incubated with mouse anti-BrdU antibody (1:500, Sigma) overnight at 4ºC in a wet chamber. Afterward, samples were incubated with FITC goat anti-mouse secondary antibody (1:100, Sigma) for 2 h at room temperature, and DAPI (1 h at room temperature) (#D3571, ThermoFisher, OR, USA). Finally, cells were observed with a fluorescence microscope (Nikon, eclipse 80i). Data were expressed as the percentages of BrdU-positive cells/DAPI positive of cells. The experiments were performed in duplicate. The results are presented as the means ± SD from three independent experiments. A total of 1,000 cells were counted per samples.

4.9 IMMUNOHISTOCHEMISTRY FOR PCNA DETECTION (PROLIFERATING CELL NUCLEAR ANTIGEN)

Cells were seeded on coverslips (24x24 mm) and fixed with 3.7% formaldehyde for 30 min. After that, the cells were washed in Tris-buffered saline (TBS; pH 7.6). Antigen retrieval was performed using Citrate Buffer Solution (0.01 mol L^{-1} and pH 6.0) for 10 min in a steam cooker. To block endogenous peroxidase, samples were treated with 3% hydrogen peroxide in Tris-buffered saline (TBS; pH 7.6) for 15 min. Coverslips were washed in TBS and submitted to a protein blocker (1% nonfat powdered milk in TBS) for 10 min. Subsequently, the material was incubated with anti-mouse monoclonal PCNA antibody (Novocastra Laboratories, Newcastle, UK) diluted 1:200 for 1 h in a sealed humidity chamber. The coverslips were rinsed in TBS and incubated with a biotinylated secondary antibody (Novostain *Super* ABC Kit - universal) (Novocastra - NCL-ABCu) for 30 min, washed again in TBS, and treated with ABC reagent (avidin-biotin-peroxidase complex; Novostain *Super* ABC Kit - universal) (Novocastra - NCL-ABCu) for 30 min. Finally, the peroxidase activity was revealed for microscopy by using DAB (3,3′-diaminobenzidine) Reveral (Spring Bioscience). The slides were counterstained with haematoxylin, mounted and documented by using a computerized image analysis (AmScope MU1000).

4.10 APOPTOSIS DETECTION BY ANNEXIN V/7-AAD

Phosphatidylserine externalization was evaluated using Kit Guava Nexin® (Merk Millipore, Massachusetts, EUA) according to manufacturer's instructions. Cells were seeded into 24-well plates at a density of 1 x 10^5 cells per well. The cell cultures were treated with PQM 277 at 5-10 μM, PQM 281 and PQM 286 at 10-20 μM or cisplatina at 20-40 μM for 24 or 48 h. The cells were collected by enzymatic digestion (Tripsin/EDTA, Sigma) and the samples were centrifuged at 1,000 rpm for 5 min at 4 °C, washed with cold PBS, and then 2 × 10^4 cells were suspended in 100 μl of DMEM. In the next step, it was added 100 μl of mix solution containing buffered Annexin V-PE and 7-AAD. The samples were read after 20 min of incubation at room temperature in a dark chamber. The analysis was performed by flow cytometry using GuavaSoft 2.7 software. The experiments were conducted in triplicate and repeated twice. Data are presented as mean ± SD.

4.11 IMMUNOBLOT

Cells were seeded into 100 mm Petri dishes at 1 × 10^6 cells/plate. The samples were treated with PQM 277 at 5-10 μM, PQM 281 and PQM 286 at 10-20 μM for 24 h. Cells were homogenized in RIPA lysis buffer (150 mM NaCl, 1.0% Nonidet P-40, 0.5% deoxycholate, 0.1% SDS and 50 mM Tris pH 8.0) containing both protease and phosphatase inhibitors (Sigma). Lysates were centrifuged (10,000 × g) for 10 min at 4 °C. Supernatants were recovered, total proteins were quantified (BCA kit, Pierce Biotechnology Inc., Rockford, IL, USA) and resuspended in Laemmli sample buffer containing 62.5 mM Tris–HCl pH 6.8, 2% SDS, 10% glycerol, 5% 2-mercaptoethanol and 0.001% bromophenol blue. An aliquot of 50 μg protein was separated by SDS–PAGE (12%) and transferred (100 V, 250 mA for 2h) onto a PVDF membrane (Amersham Bioscience), blocked for 1h at 4°C with blocking solution [5% non-fat milk in Tris-buffered saline (TBS) + 0.1% (v/v) Tween20] to prevent nonspecific protein binding. The membrane was probed with primary antibodies: anti-phospho-ERK(Tyr 204) (Santa-Cruz, sc-7383, 1:200), anti-ERK 1/2 (Cell signaling, #4696, 1:1000), anti-Cyclin B1 (Santa Cruz, sc-245, 1:200), anti-AKT(Ser 473) (Cell signaling, #4060), and α-tubulin (Sigma– 1:1000) overnight at 4^{o}C. After washing with TBS-tween (0.1%), the membrane was incubated with a secondary antibody (anti-rabbit peroxidase conjugated) for 2h at room

temperature. Immunoreactive bands were visualized with the ECL Western Blotting Detection Kit (Amersham Pharmacia). A reprobing protocol was followed for detecting immunoreactive bands for different antibodies. Results were obtained from three independent experiments. The quantification of immunoreactive bands was performed using a public program (Bio-Rad software).

4.12 COMET ASSAY

Alkaline comet assay was performed as described previously by Singh *et al*. (1988), with some modifications. Briefly, cells were seeded in tissue culture flasks and incubated for 12 and 24 h with PQM 277 at 10 µM. After treatment, the cells collected by enzymatic digestion, and cell viability was checked by Trypan blue exclusion assay. All treated cultures showed greater than 70% of viability. Two hundred thousand viable cells were suspended in 100 µL of 0.5% low melting point agarose (Sigma-Aldrich) at 37 °C and mixture was spread into microscope slides pre-coated with 1.5% normal-melting point agarose (Sigma-Aldrich). Next, the samples were immersed in cold (4 °C) lysis solution (1% Triton X-100, 10% DMSO, 2.5 mM NaCl, 100 mM Na2EDTA, 100 mM Tris, pH 10) for 24 h and electrophoresis was performed (25 V, 300 mA for 25 min). After neutralization (0.4 M Tris–HCl, pH 7.5 for 15 min) and fixation (ethanol), the samples were stained with SYBR® Green I solution (Invitrogen by Thermo Fisher Scientific Inc., Rockford, IL, USA) diluted 1:100 in 1 × PBS and analyzed by fluorescence microscope using a 20 × objective. The images were captured and analyzed using the ImageJ open comet program (ImageJ, Wayne Rasband, National Institutes of Health, USA) to demarcate the "head" and the "tail" regions of each comet. UV was used as a positive control. Fifty randomly selected nuclei were analyzed per slide. The extent of DNA damage (tail moment) was expressed as the mean ± SD from three independent experiments.

4.13 TRANSCRIPT LEVEL EVALUATION

Real-time PCR was performed according to Lamartine-Hanemann *et al*. (2020). Briefly, the cells were seeded into 6-well plates at a density of 1 x 10^5 cells per well. Samples were treated with PQM 277 at 5 or 10 µM for 24 h. Total RNA was extracted using the RNeasy® Mini kit (Qiagen, Mississauga, ON, Canada) and RNA concentrations were measured by spectrophotometer using a NanoDrop® ND 1000 (Thermo Scientific, Wilmington, DE, USA).

Then, 1 µg of total RNA was incubated with DNase I (1 U/µg; Invitrogen, São Paulo, SP, Brazil) and subjected to reverse transcription using random primers and the High Capacity cDNA Reverse Transcription Kit® (Applied Biosystems, São Paulo, SP, Brazil).

Expression of the target genes (Table 1) was investigated by real-time PCR with an ABI 7500 thermocycler using Power Sybr Green PCR Master Mix (Applied Biosystems). The genes were amplified using the following conditions: 95 °C for 10 min (1 cycle), denaturation at 95 °C for 10 s, and annealing and extension at 60 °C for 1 min (40 cycles). To select the most stable housekeeping gene, β-actin (ACTB), glyceraldehyde-3- phosphate dehydrogenase (GAPDH), and 18S ribosomal RNA (18srRNA) amplification profiles were compared using the geNorm applet for Microsoft Excel (medgen.ugent.be/genorm; Vandesompele *et al.* (2002); the most stable housekeeping gene was ATCB. The relative abundance of each target gene was calculated using the ΔΔCt method with efficiency correction and a control sample for calibration (Pfaffl, 2001). Each sample was run in triplicate and non-template control was included. The data are presented as mean ± standard error of the mean (SEM) from three independent experiments.

Table 1- Information of primers used for amplification in real-time PCR.

Gene	Sequence	Reference
CDKN1A	F 5'- CCATAGCCTCTACTGCCACCATC-3'	NM_001291549.1
	R 5'- GTCCAGCGACCTTCCTCATCCA-3'	
CCNB1	F 5'- GTACCCTCCAGAAATTGGTGA-3'	NM_031966.2
	R 5'- GACTACATTCTTAGCCAGGTG-3'	
NRF2	F 5'- CAATGAGGTTTCTTCGGCTACG -3'	NM_006164.4
	R 5'- AAGACTGGGCTCTCGATGTG -3'	
CHK2	F 5'- CCCAAGGCTCCTCCTCACA -3'	NM_007194.3
	R 5'- AGTGAGAGGACTGGCTGGAGTT -3'	
Aur A	F 5'- TCTTCACAGGAGGCAAATCCA-3'	XM_017028035.1
	R 5'- AATAAGTTACACACTCACTCAGGTACTA-3'	
Aur B	F 5'- AAAGAGCCTGTCACCCCATC-3'	XM_017025310.1
	R 5'- CGCCCAATCTCAAAGTCATC-3'	
BAX	F:5'- TTCCTTACGTGTCTGATCAATCC-3'	NM_004324.3
	R:5'- GGGCAGAAGGCACTAATCAA -3'	
BCL-2	F:5'- CAGAAGTCTGGGAATCGATCTG -3'	NM_000657.2
	R:5'- AATCTTCAGCACTCTCCAGTTATAG -3'	
ACTB	F 5'- AGAGCTACGAGCTGCCTGAC-3'	NM_001101.3
	R 5'- AGCACTGTGTTGGCGTACAG-3'	
GAPDH	F 5'- GGATTTGGTCGTATTGGGC-3'	NM_002046.4
	R 5'- TGGAAGATGGTGATGGGATT-3'	
18srRNA	F 5'- GTAACCCGTTGAACCCCATT-3'	HQ387008.1
	R 5'- CCATCCAATCGGTAGTAGCG-3'	

F = forward primer; R = reverse primer
Source: From the author

4.14 STATISTICAL ANALYSIS

The results were tested for significance using test t or one-way analysis of variance (ANOVA) followed by Dunnet's post-test using GraphPad Prism®. The values are expressed as mean ± SD from at least three independent experiments.

5 RESULTS

5.1 ANTIPROLIFERATIVE POTENTIAL OF PIPERINE-CHLOROGENIC ACID HYBRIDS ON MELANOMA CELLS

Cell viability was determined on different melanoma cell lines treated for 48 h with different substances at 25 µM. We observed that SK-MEL-147 cell line was more responsive to tested compounds than CHL-1 or WM-1399 cell lines (Figure 2). Reduced cell viability rates were observed in SK-MEL-147 cultures treated with PQM 277, PQM 281, PQM 285, PQM 286, PQM 287 and PQM 288 (Figure 2), however PQM-277 showed to be the most active compound. We did not observe reduction in cell viability rate in SK-MEL-147 cultures treated with parent compounds (**1**) or (**2**), in the same experimental conditions evaluated for synthesized compounds (Figure 2). Likewise, a significant reduction in cell viability was not observed in samples treated with physical mixture of piperine and chlorogenic acid (Figure 2). In this study, primary dermal fibroblast (FBM) was included to evaluate cytotoxic potential of tested substances on normal cells. Cell viability rates were not significantly reduced in FBM cultures treated with PQM-277-PQM-288 (Figure 2).

Based on screening data, dose-response curves were performed to determine the IC_{50} values (concentration that inhibits 50% of cell growth) for active substances on SK-MEL-147 (Figure 3A and Table 2). The PQM 277 displayed lower IC_{50} value (12.82 ± 0.81) compared to other tested substances. In addition, the ability of the PQM 277 to reduce viability rate of SK-MEL-147 cells was higher than those observed for cisplatin (IC_{50} value = 19.54 ± 1.10), a powerful cytotoxic antineoplastic agent (Table 2). The IC_{50} values of these compounds were not determined on FBM (primary dermal fibroblast) once cell viability was minimally affected after 48 h of treatment (Table 2). Based on preliminary data, PQM 277, PQM 281 and PQM 286 and SK-MEL-147 were selected for further investigations.

The clonogenic assay was performed to evaluate to ability of PQM 277, PQM 281 and PQM 286 to inhibit cell proliferation of SK-MEL-147 for prolonged period. We observed significant reduction of colonies number in all samples treated compared to control groups, however, PQM-286 showed to be the more potent than PQM-277 or PQM-281 to inhibit clonogenic ability of the SK-MEL-147 cells (Figures 3B, 3C and 3D).

Figure 2- Cell viability determined by sulforhodamine B (SRB) after 48 hours of treatment at 25 µM with the different PQM (277-288), piperin, chlorogenic acid, cisplatin,and temozolomide. ***p < 0.001 according ANOVA followed by Dunnet post-test. DMSO (0.1% v/v) was used as negative control.

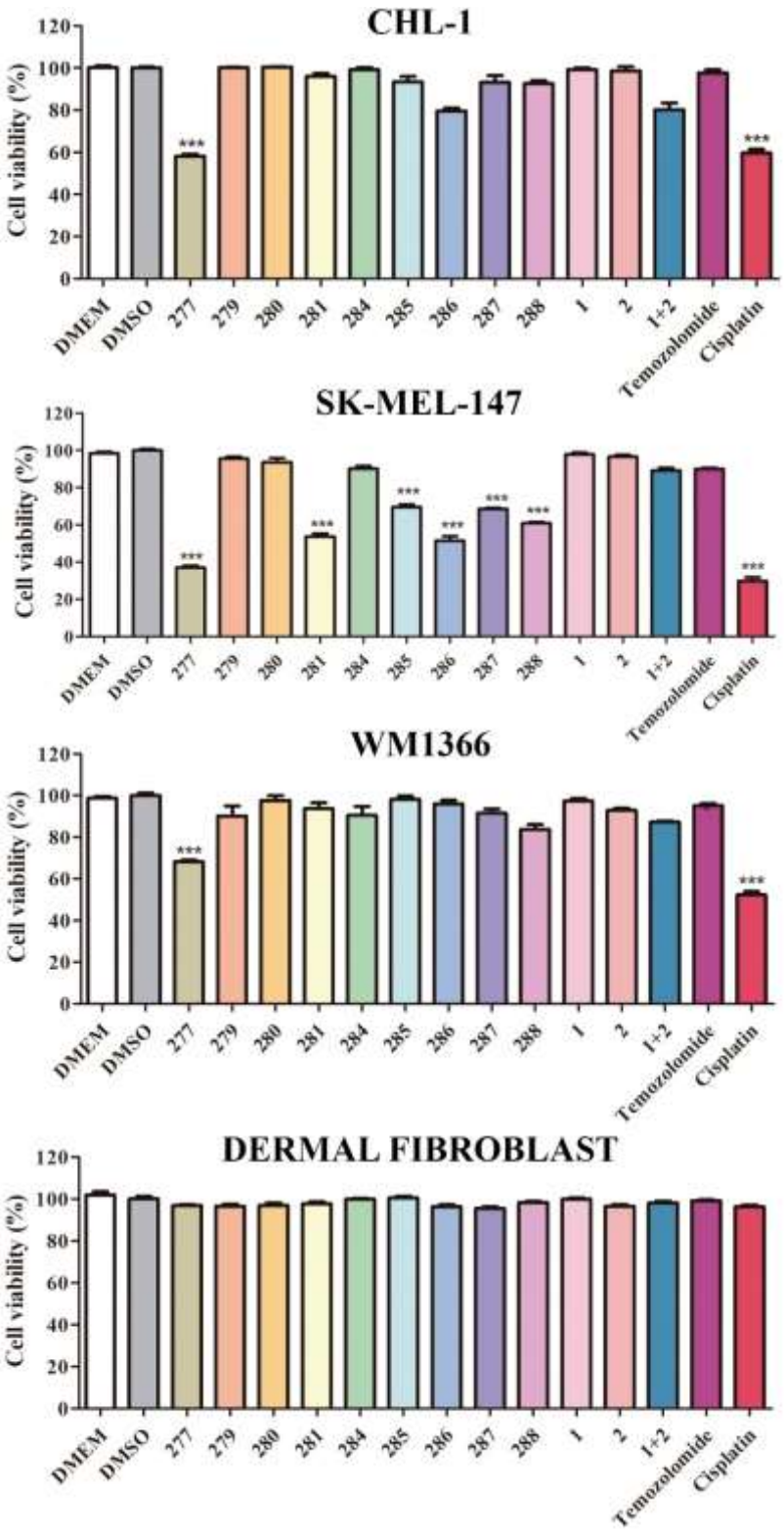

Source: From the author

Figure 3- Cell viability determined Sulforhodamine B and clonogenic assay analysis.

.

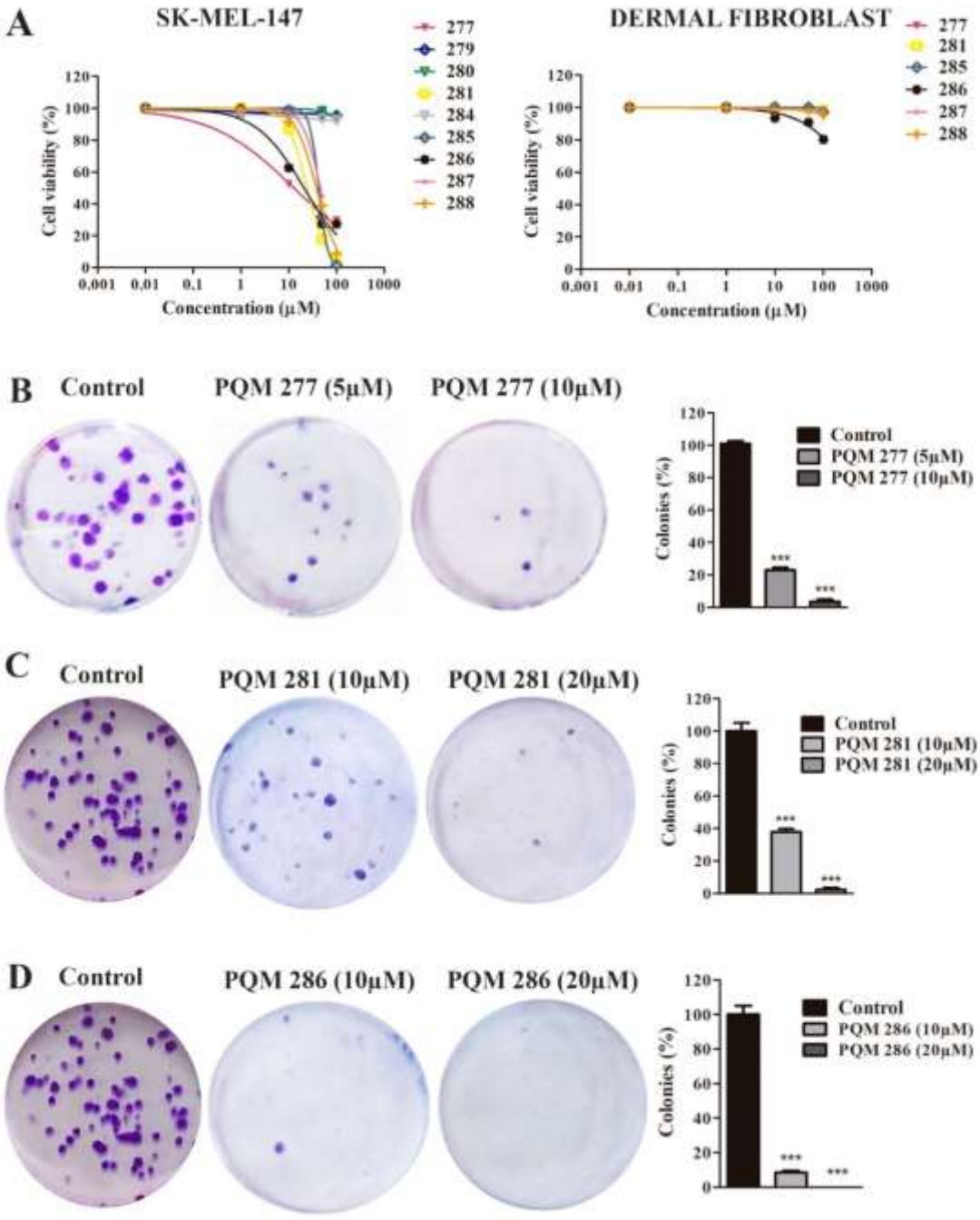

Source: From the author

Note: (A) Cell viability determined Sulforhodamine B after 48 hours of treatment. PQM substances were evaluated on SK-MEL-147 cells and dermal fibroblast cultures. (B) Illustrative images and clonogenic assay analysis with compound PQM 277 at 5 and 10 µM for 24 h. (C) Illustrative images and clonogenic assay analysis with compound PQM 281 at 10 and 20 µM for 24 h. (D) Illustrative images and clonogenic assay analysis with compound PQM 286 at 10 and 20 µM for 24 h. SK-MEL-147 cells were treated with compounds and recovered in fresh medium for additional 12 days. ***$p<0.001$ according to ANOVA followed by Dunnet post-test.

Table 2- IC_{50} values (μM) determined from the Sulforhodamine B assay. Cell cultures were treated with different substances for 48 h.

	SK-MEL-147	Dermal fibroblast**
PQM 277	12.82 ± 0.81	ND
PQM 279	ND	ND
PQM 280	ND	ND
PQM 281	24.42 ± 0.42	ND
PQM 284	ND	ND
PQM 285	42.42 ± 0.84	ND
PQM 286	20.95 ± 1.98	ND
PQM 287	45.82 ± 0.70	ND
PQM 288	37.81 ± 1.34	ND
Cisplatin*	19.54 ± 1.10	ND
Temozolomide	ND	ND

Source: From the author

Note: *Cisplatin was used as a positive control. ** non-tumor cell line (primary dermal fibroblast). ND: not determined once cell viability was not sufficiently reduced to determine IC_{50} values.

5.2 MOLECULAR MECHANISMS UNDERLYING ANTIPROLIFERATIVE AND PRO-APOPTOTIC EFFECTS OF PQM 277 ON SK-MEL-147

Subsequently, the cell cycle analysis was performed to evaluate whether PQM 277 on SK-MEL-147 induces cell cycle arrest. We observed that PQM 277 drastically affected cell cycle progression. There was significant increase in G2/M population with reduced frequency of cells in S-phase in samples treated with PQM 277 for 24 h compared to control samples (Figures 4A and 4B). There was also increase in the Sub-G1 population in samples treated with PQM 277 at both concentrations (5 and 10 μM) compared to the control groups (Figures 4A and 4B).

To validate the results obtained in the cell cycle analysis, we used a specific marker of S-phase. The bromodeoxyuridine incorporation assay was carried out to determine S-phase population. We observed reduced frequency in S-phase population in treated samples when compared to control groups (Figure 4C). In addition, mitotic index was also determined in cytological preparations immunolabeling for α-tubulin and stained with DAPI (Figures 6A and 6B). The results showed that PQM 277 treatment significantly increased the frequency of cells in mitosis (Figure 6B) when compared to the control. Importantly, the frequency of cells in prometaphase and metaphase in samples treated with PQM 277 was higher compared to control groups (Figure 6B), and microtubules network was drastically altered in treated samples (Figure 6A).

To investigate potential molecular targets involved in the antiproliferative/cytotoxic activity of PQM 277, we investigated the expression profiles at mRNA level and expression profiles at protein levels by Western blotting of critical regulators at G2/M transition (LAPENNA; GIORDANO, 2009; MATTHEWS; BERTOLI; BUIN, 2022). Thus, the expression profiles of *CDKN1A* (p21), *CCNB1* (cyclin B1) and *CDK1* were analyzed by qPCR, while cyclin B expression levels and p21 were determined by western blotting and immunolabeling. The relative expression of mRNA for *CCNB1* and *CDK1* were lower in the samples treated with PQM 277 for 24 h (Figure 4D). Additionally, cyclin B protein expression was significantly reduced in samples treated with PQM 277 at 5 µM for 24 h (Figures 4E) compared to control groups. We found a significant augment in the frequency of positive cells for p21 in cultures treated with PQM 277 at 5 and 10 µM for 24 h compared to control groups, which localization was exclusively nuclear (Figures 5A and 5B). In addition, a higher mRNA abundance of *CDKN1A* was observed in cultures treated with PQM 277 at 5 and 10 µM for 24 h compared to control group (Figure 5C).

Further, we also investigated gene expression profiles of *Aurora A*, *Aurora B* and *PLK1*, which are also involved in G2/M transition, to confirm the role of the compound PQM 277 as an antiproliferative agent. We found reduced abundance of mRNA for *Aurora A*, *Aurora B* and *PLK1* in treated samples compared to the control group (Figure 6C). These additional data reinforce therefore that compound PQM 277 inhibits proliferation of SK-MEL-147. This effect was associated to its ability to modulate critical regulators of cell cycle progression.

Figure 4- Cell cycle analysis, BrdU immunodetection, mRNA expression determined by qPCR and protein expression levels.

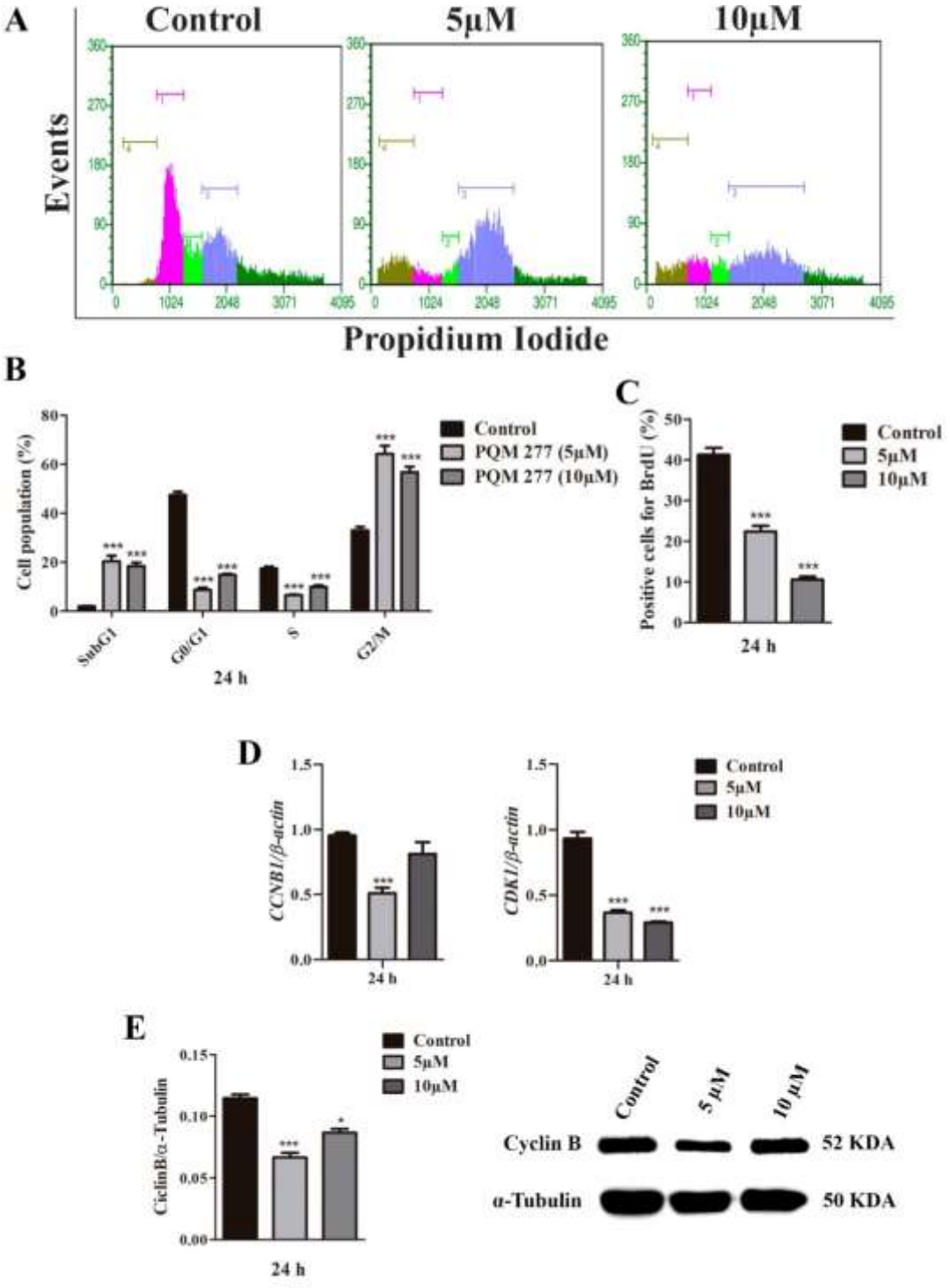

Source: From the author

Note: SK-MEL-147 cultures were treated for 24 h with PQM 277 at 5 and 10 µM. (A and B) Representative histograms obtained by flow cytometry and cell cycle analysis. Sub-G1 (brown), G0/G1 (pink), S (green), G2/M (blue), hypertetraploid population (dark green). (C) BrdU immunodetection indexes determined after 24 h treatment. (D) Relative mRNA expression determined by qPCR (E) Protein expression levels of Cyclin B. α-tubulin was used as a loading controls.*$p<0.05$ and ***$p<0.001$ according to ANOVA followed by Dunnet post-test.

Figure 5- p21 immunoreaction pattern, frequency of cell positive for p21 and mRNA expression.

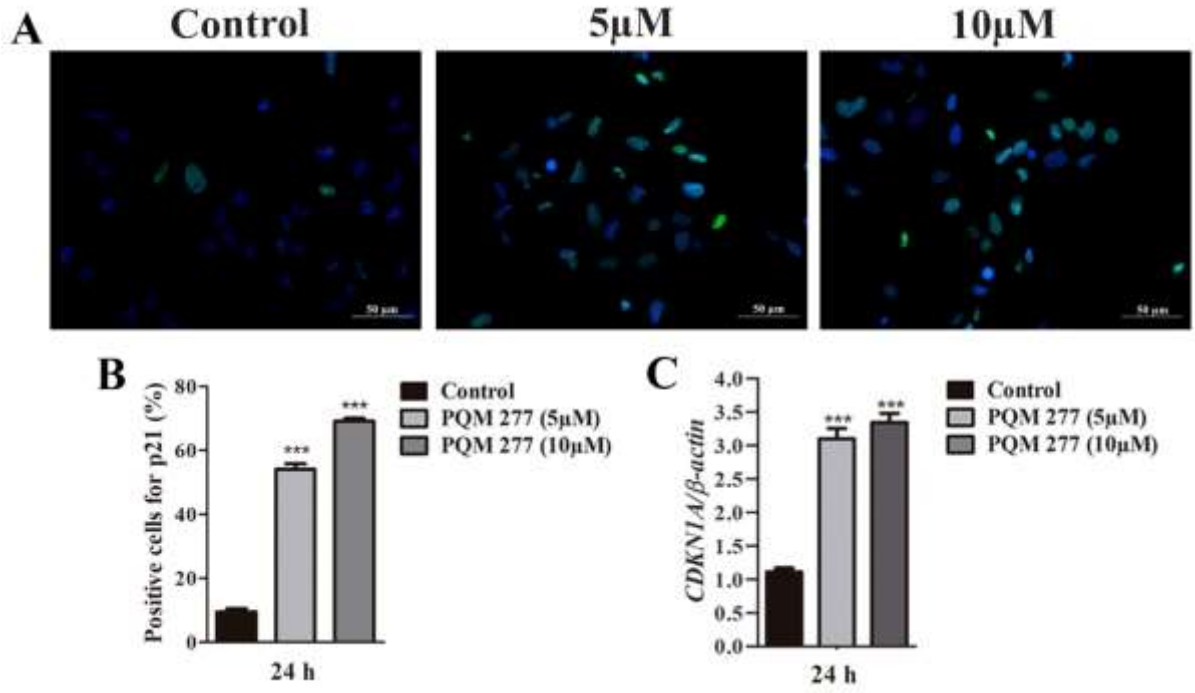

Source: From the author

Note: SK-MEL-147 cell cultures were treated with PQM 277 at 5 and 10 µM for 24 h. (A) Representative images exhibiting p21 immunoreaction pattern. (B) Frequency of cell positive for p21. (C) Relative mRNA expression determined by qPCR. *** $p<0.001$ according to ANOVA followed by Dunnet post-test.

Figure 6- Microtubule network, mitotic indexes and mRNA expression determined by qPCR.

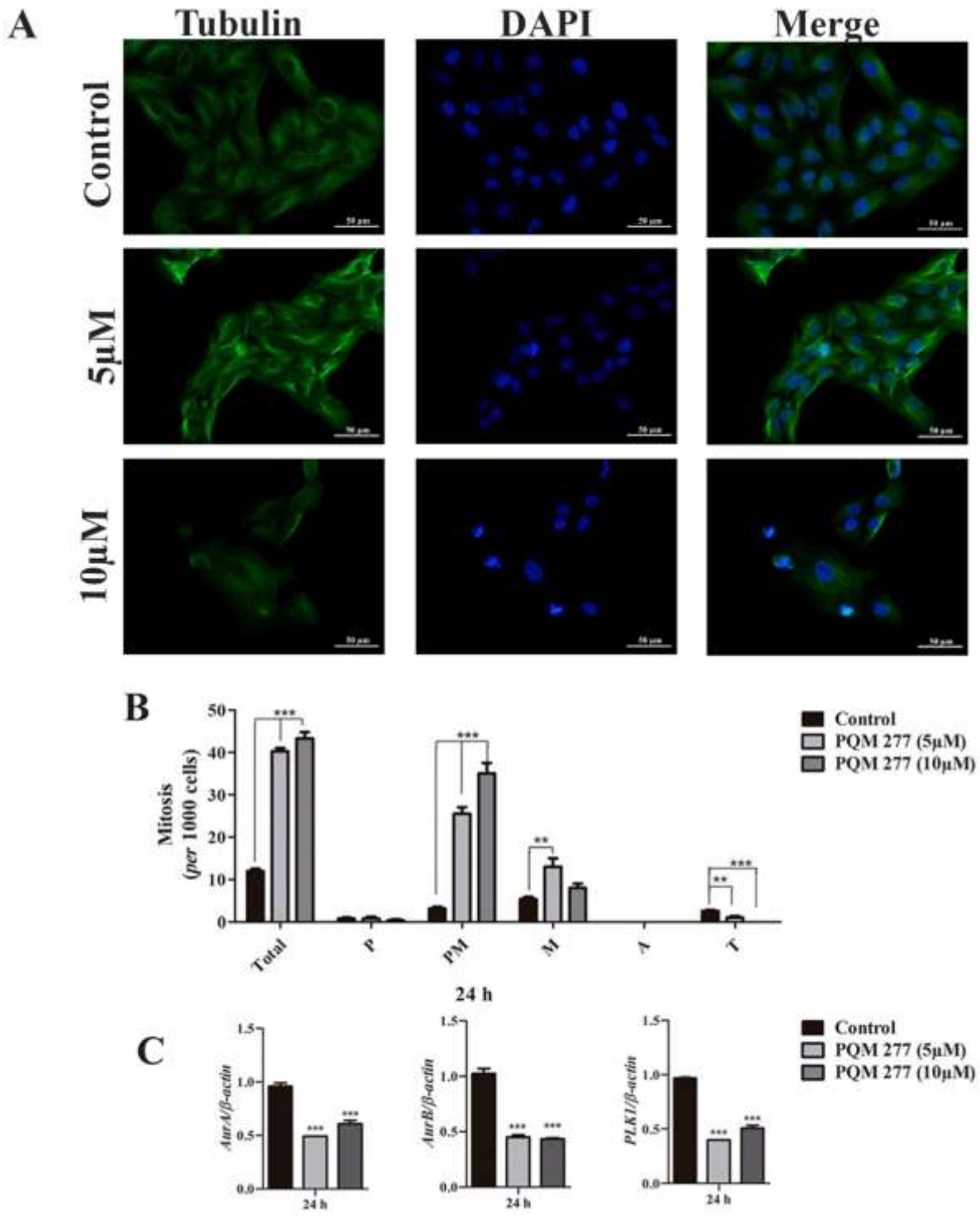

Source: From the author

Note: SK-MEL-147 cultures treated with compound PQM 277 at 5 and 10 µM for 24 h. (A) Illustrative imagens exhibiting microtubule network evidenced by anti-α-tubulin (green). (B) Mitotic indexes determined by counting the mitosis from cytological preparations labeled with DAPI and anti-α-tubulin. (C) Relative mRNA expression determined by qPCR in. **p<0.01 and *** p<0.001 according to ANOVA followed by Dunnet post-test.

Figure 7- Protein expression levels determined by immunoblotting.

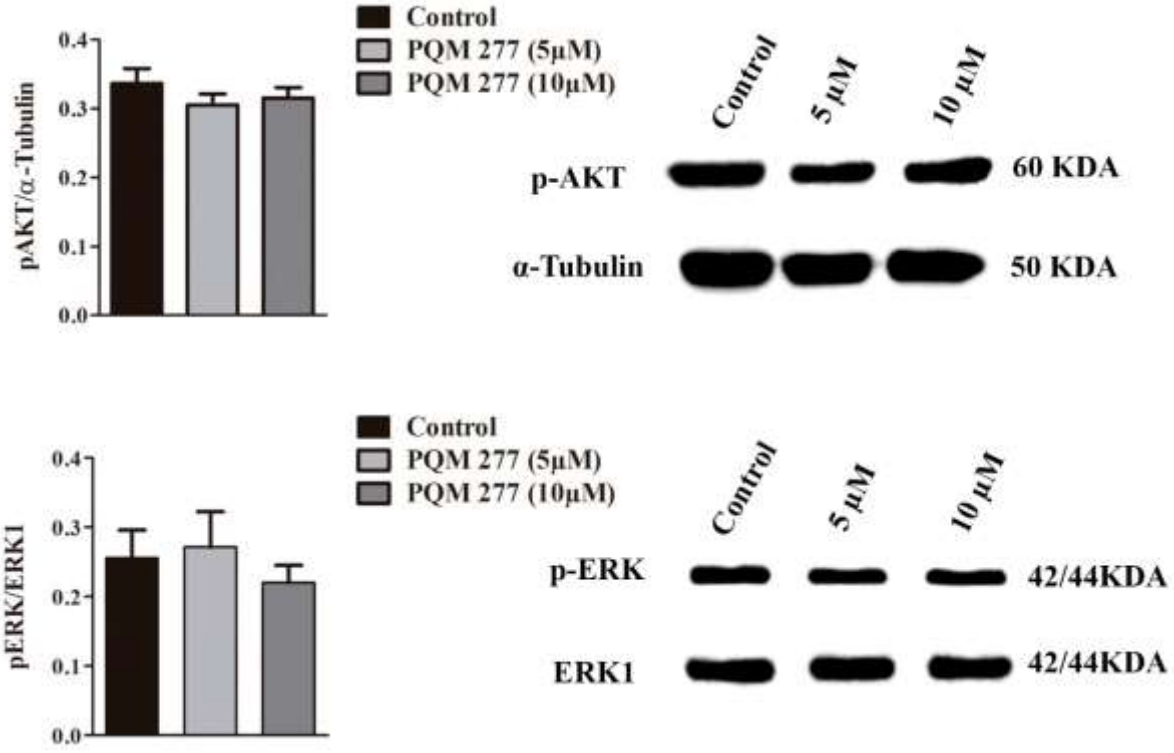

Source: From the author
Note: SK-MEL-147 cells were treated for 24 h with compound PQM 277 at 5 and 10 µM and protein expression levels were determined by immunoblotting. α-tubulin and ERK1/2 were used as a loading controls.

We sought to evaluate the expression profile of the p-ERK and p-AKT, However, we did not observe any significant alteration at protein levels of these signaling protein in the tested experimental conditions (Figure 7).

Based in increased sub-G1 population previously observed in cell cycle analysis (Figure 4A and 4B), we evaluated pro-apoptotic potential of PQM 277 on SK-MEL-147 cells using annexin V assay. We found increased frequency of positive cells for annexin V in samples treated with PQM 277 at 5 and 10 µM for 24 and 48 h compared to the control group, indicating that cytotoxic activity of PQM 277 on SK-MEL-147 is associated to its ability to induce apoptosis (Figures 8A and 8B). In this experimental approach, we used cisplatin as positive control at 20 and 40 µM. Further, we analyzed the mRNA abundance of *BCL-2* and *BAX*. The treatment with PQM 277 at 5 and 10 µM for 24 h presented higher mRNA levels of *BAX* compared to control group with significant reduction mRNA for *BCL-2* indicating that PQM 277 induced *BAX*-upregulation and *BCL-2*-downregulation (Figures 8C).

Figure 8- Annexin V/7-AAD and relative mRNA expression determined by qPCR.

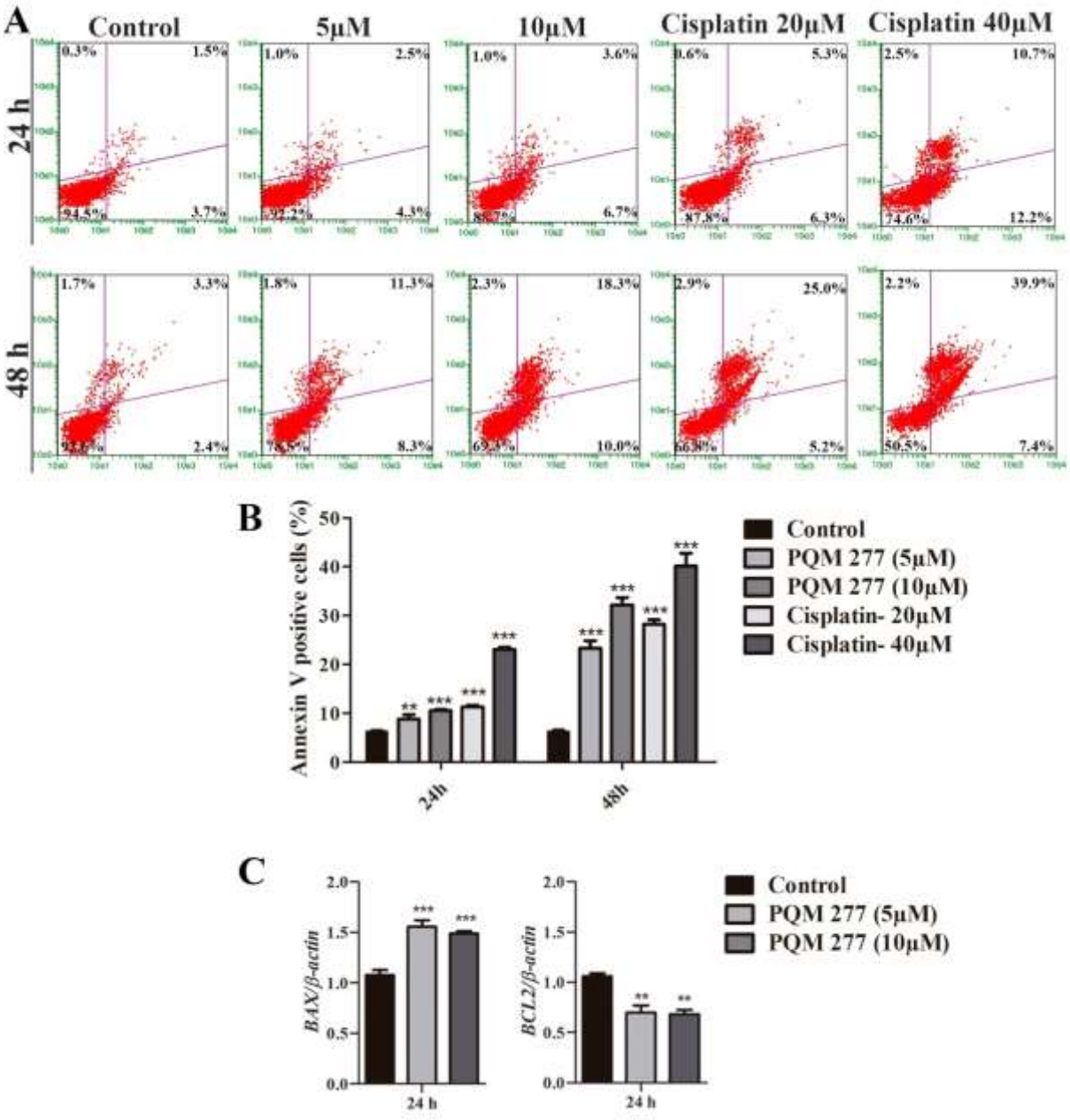

Source: From the author

Note: (A and B) Representative dot plots and analysis of annexin V/7-AAD assays performed in SK-MEL-147 cultures after 24 and 48 h after treatment with PQM 277. Viable cells (lower left quadrants), early apoptosis (lower right quadrants), late apoptosis (upper right quadrants), and necrotic cells (upper left quadrants). (C) Relative mRNA expression determined by qPCR in SK-MEL-147 cultures treated with compound PQM 277 at 5 and 10 µM for 24 h. **p<0.01 and *** p<0.001 according to ANOVA followed by Dunnet post-test.

We investigated whether pro-apoptotic activity of PQM 277 on studied cell line is related to its ability of inducing DNA damage. The results from comet assay showed that the treatment

with PQM 277 at 10 μM for 12 and 24h did not induce DNA fragmentation. There was not significant differences was not observed in treated samples compared to control groups. Cells irradiated with ultraviolet (UV) light were used as positive controls in this experimental approach (Figures 9A and 9B). In parallel, we also evaluated mRNA abundance of checkpoint kinase 2 (*CHK2)* and nuclear factor-erythroid 2-related factor 2 (*NRF2).* Our results showed that treatments at 5 and 10 μM for 24 h with PQM 277 did not change mRNA levels of *NRF2* compared to control, however, *CHK2* mRNA levels were lower in treated samples (Figure 9C). Therefore, the data indicate that cell cycle arrest induced by PQM 277 on SK-MEL-147 is not associated to its ability to induce DNA damage.

Figure 9- Comet assay analysis andrRelative mRNA expression determined by.

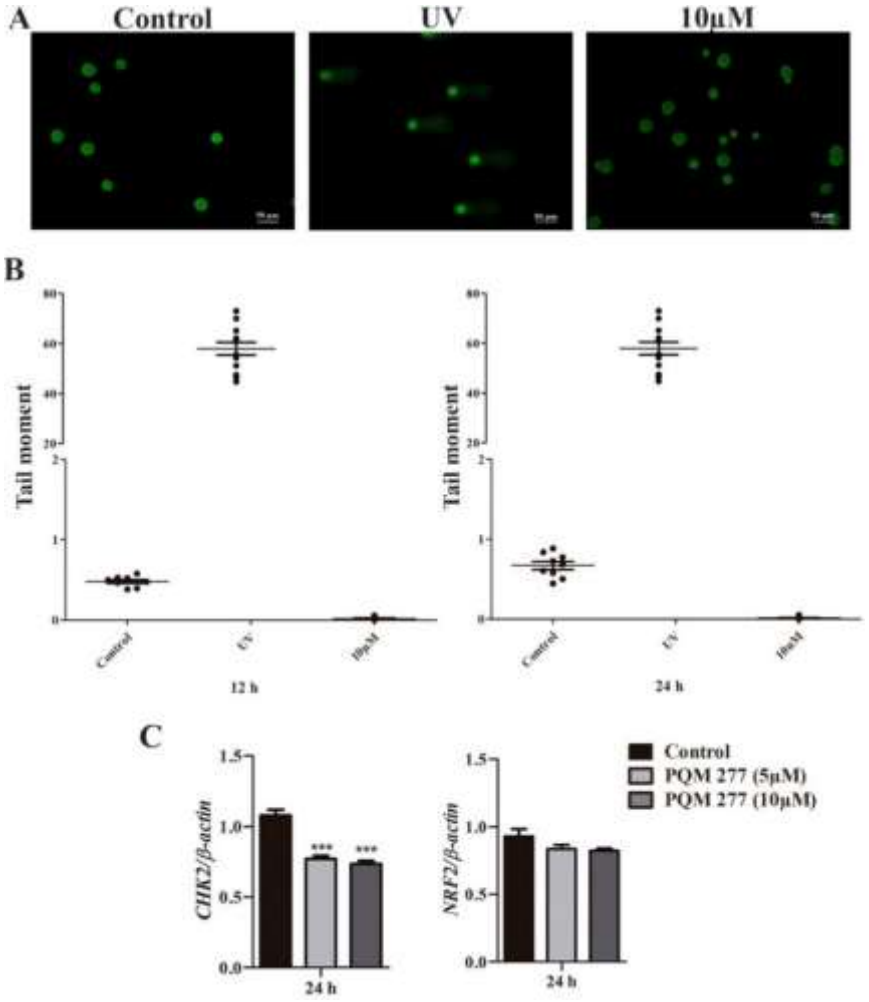

Source: From the author

Note: (A and B) Comet assay analysis showing DNA damage indexes after 12-24 h of treatment. UV radiation was used to induce DNA damage. (C) Relative mRNA expression determined by qPCR in SK-MEL-147 cultures treated with compound PQM 277 at 5-10 μM for 24 h. *** $p<0.001$ according to ANOVA followed by Dunnet post-test.

5.3 MOLECULAR MECHANISMS UNDERLYING ANTIPROLIFERATIVE AND PRO-APOPTOTIC EFFECTS OF PQM 281 AND PQM 286 ON SK-MEL-147 CELLS

We also performed cell cycle analysis to determine whether PQM 281 and PQM 286 also induces G2/M arrest on SK-MEL-147, as well as was found for PQM 277. Our results showed that antiproliferative activity of PQM 281 and PQM 286 are associated to distinct molecular mechanism when compared to PQM 277. G0/G1 populations were significantly increased by PQM 281 and PQM286 treatments, while the frequencies of cells in the S-phase were reduced. We also found increase in the Sub-G1 population in cell cultures treated with these compounds at 10 and 20 μM indicating the occurrence of cell death (Figures 10-11A and 10-11B).

Next, we determined the frequency of cells in the S phase using PCNA marker. The treatment with PQM 281 and PQM 286 at 10 and 20 μM significantly reduced the number of PCNA positive cells compared to control groups (Figures 10C and 11C). These data reinforce those obtained by flow cytometry.

We also sought to investigate the molecular mechanism associated with ability of PQM 281 and PQM 286 to inhibit cell cycle arrest at G1/S transition (BERTOLI; CAVA; CASTIGLIONI, 2015; LAPENNA; GIORDANO, 2009; MATTHEWS; BERTOLI; BUIN, 2022). Thus, expression profiles of regulatory proteins at G1/S transition were determined by western blotting. The relative expression of cyclins D and E was significant reduced in samples treated with PQM 281 at 10 and 20 μM for 24h h (Figure 10D). However, we did not observe significant difference in cyclins levels in samples treated with PQM 286 compared to control group (Figure 11D).

Figure 10- Cycle analysis, PCNA immunodetection and protein expression profiles.

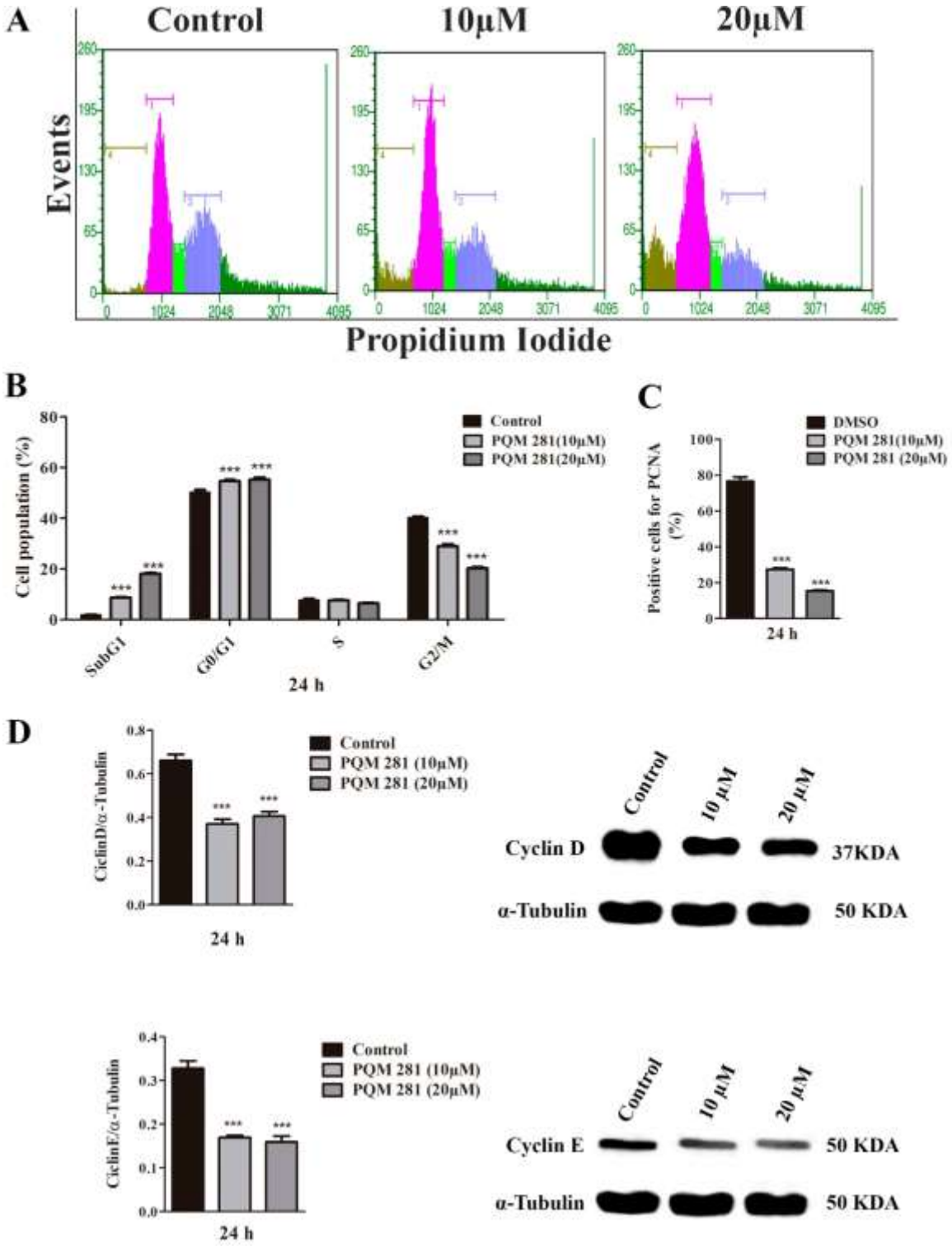

Source: From the author

Note: Cells were treated for 24 h with PQM 281 at 281 at 10 or 20 µM. (A and B) Representative histograms obtained by flow cytometry and cell cycle analysis. Sub-G1 (brown), G0/G1 (pink), S (green), G2/M (blue), hypertetraploid population (dark green). (C) PCNA immunodetection indexes. (D) Protein expression profiles of cyclins D and E. α-tubulin was used as a loading controls. ***$p<0.01$ according to ANOVA followed Dunnet post-test.

Figure 11- Cycle analysis, PCNA immunodetection and protein expression profiles.

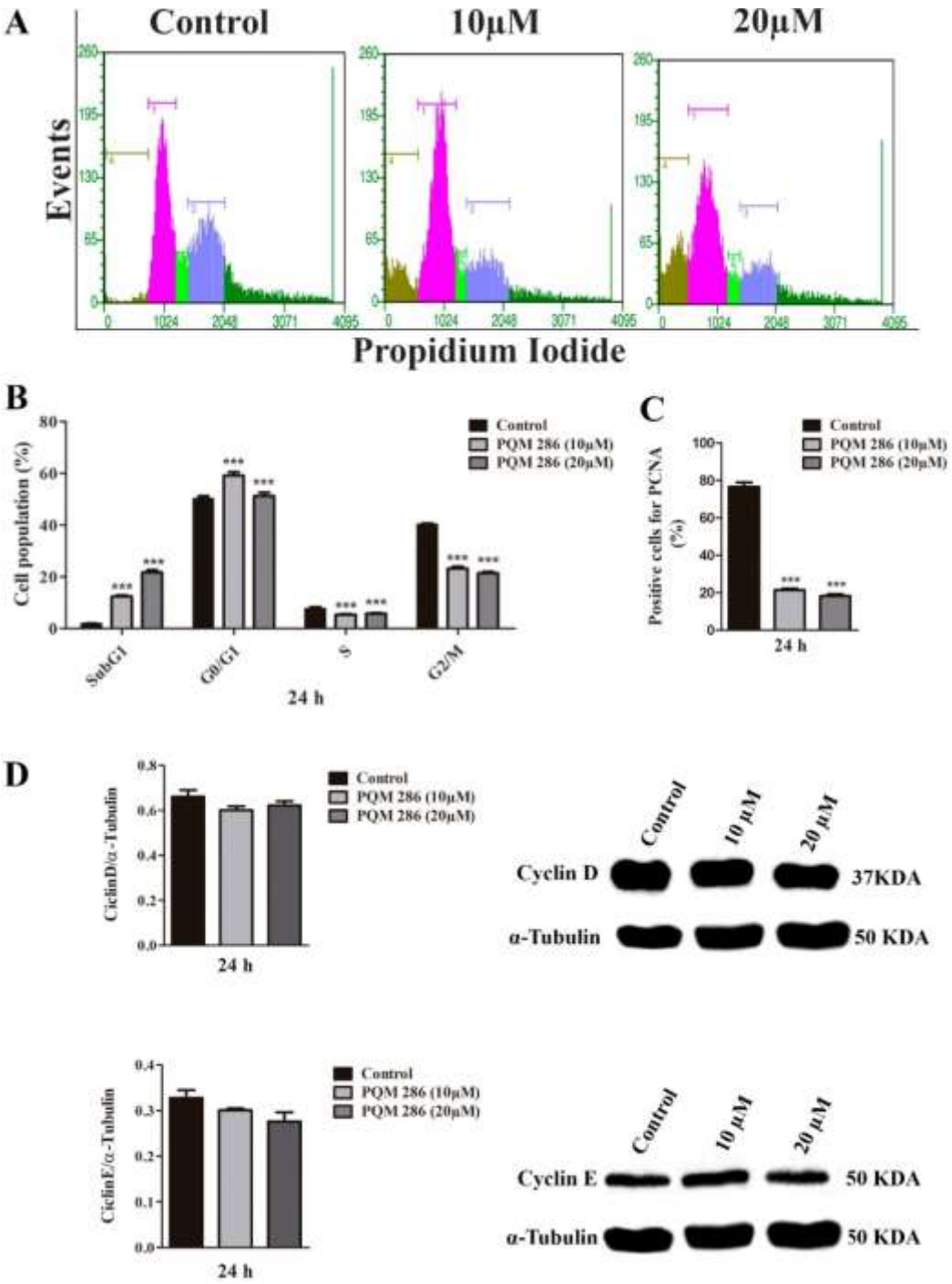

Source: From the author

Note: SK-MEL-147 cultures were treated for 24 h with PQM 286 at 10 and 20 µM. (A and B) Representative histograms obtained by flow cytometry and cell cycle analysis. Sub-G1 (brown), G0/G1 (pink), S (green), G2/M (blue), hypertetraploid population (dark green). (C) Proliferating cell index determined by PCNA immunodetection. (D) Protein expression profiles f cyclins D and E. α-tubulin was used as a loading controls. ***p<0.01 according to ANOVA and Dunnet post-test.

The expression profile of the p-ERK and p-AKT were also evaluate in SK-MEL-147 cell cultures treated with PQM 281 and PQM 286. Our results showed that PQM 281 induced increase of p-ERK at 20 µM, but no differences were observed regarding p-AKT (Figure 12). Conversely, PQM 286 at 10 and 20 µM induced p-AKT downregulation, and p-ERK expression was higher in samples treated with PQM 286 at 10 µM when compared to control group (Figure 13).

Figure 12- Protein expression profiles of p-AKT and p-ERK.

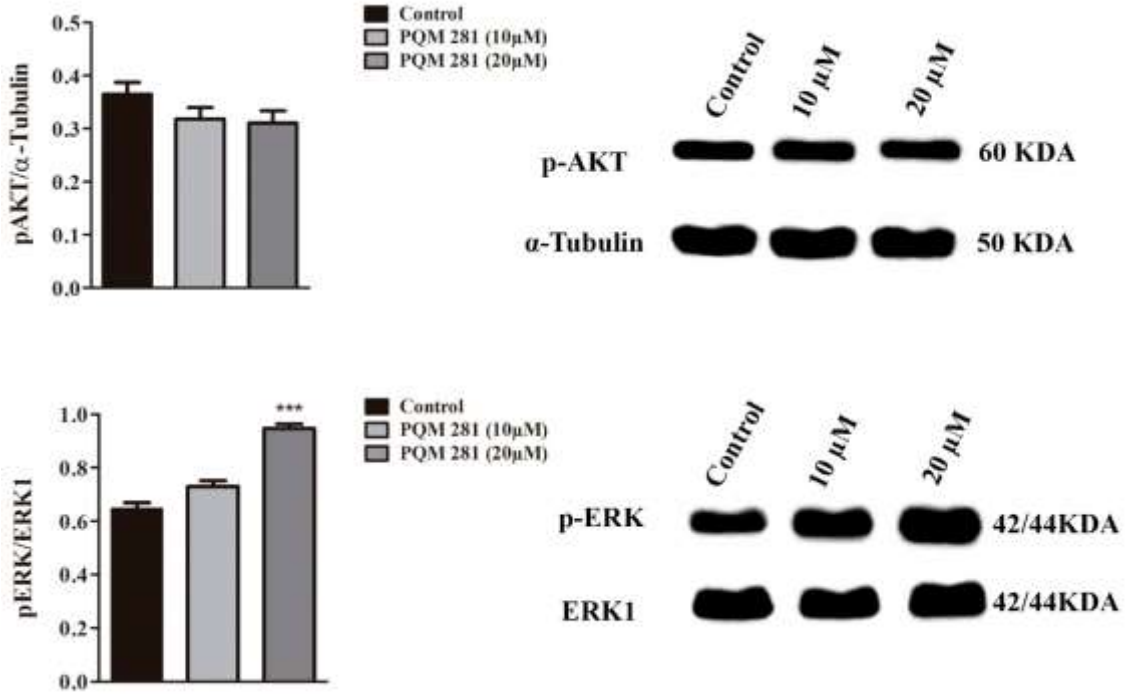

Source: From the author

Note: SK-MEL-147 cells were treated for 24 h with compound PQM 281 at 10 and 20 µM and protein expression profiles of p-AKT and p-ERK were determined by immunoblotting. α-tubulin and ERK1/2 were used as a loading controls. *** $p<0.001$ according to ANOVA followed by Dunnet post-test.

Figure 13- Protein expression profiles of p-AKT and p-ERK.

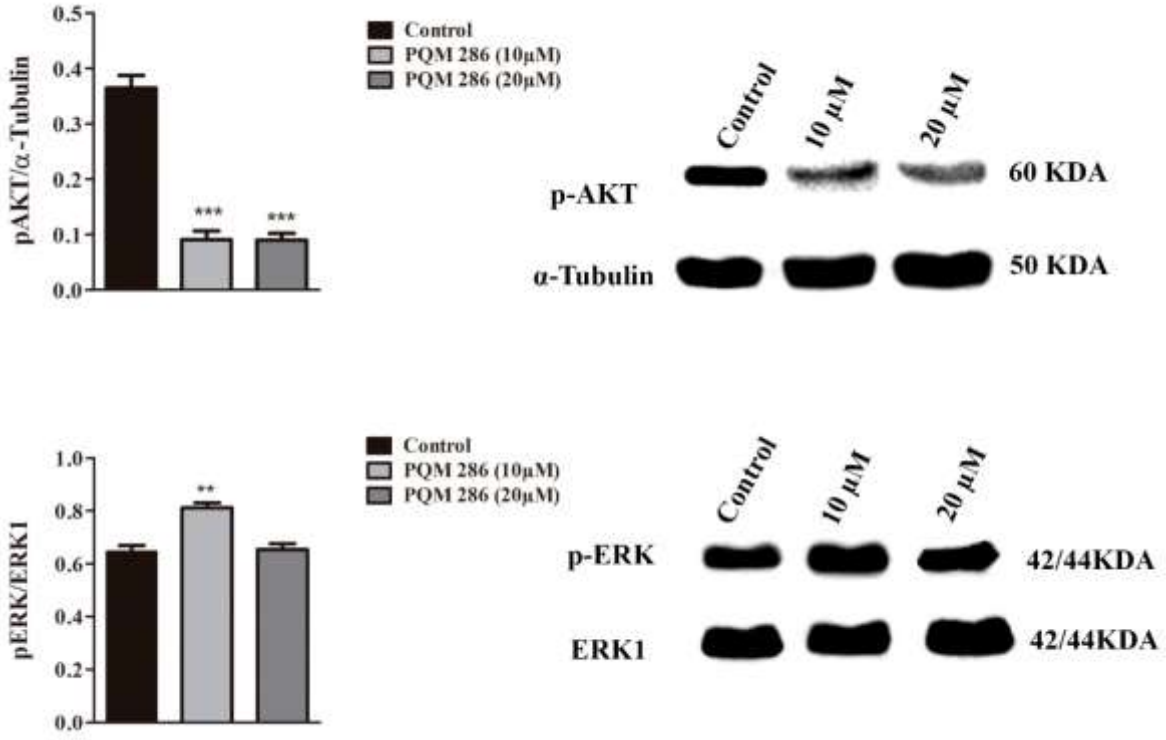

Source: From the author

Note: SK-MEL-147 cells were treated for 24 h with compound PQM 286 at 10 and 20 μM and protein expression profiles were determined by immunoblotting α-tubulin and ERK1/2 were used as loading controls. **p<0.01 and *** p<0.001 according to ANOVA followed by Dunnet post-test.

Considering the increased sub-G1 population found in cell cycle analysis (Figure 10-11A and 10-11B), the pro-apoptotic potential of PQM 281 and PQM 286 were evaluated using annexin V assay. We observed increased frequency of positive cells for annexin V all treated groups compared to the control samples (Figures 14 and 15). In this experimental approach, we used cisplatin as positive control at 40 μM.

Figure 14- Annexin V/ propidium iodide (PI) assays.

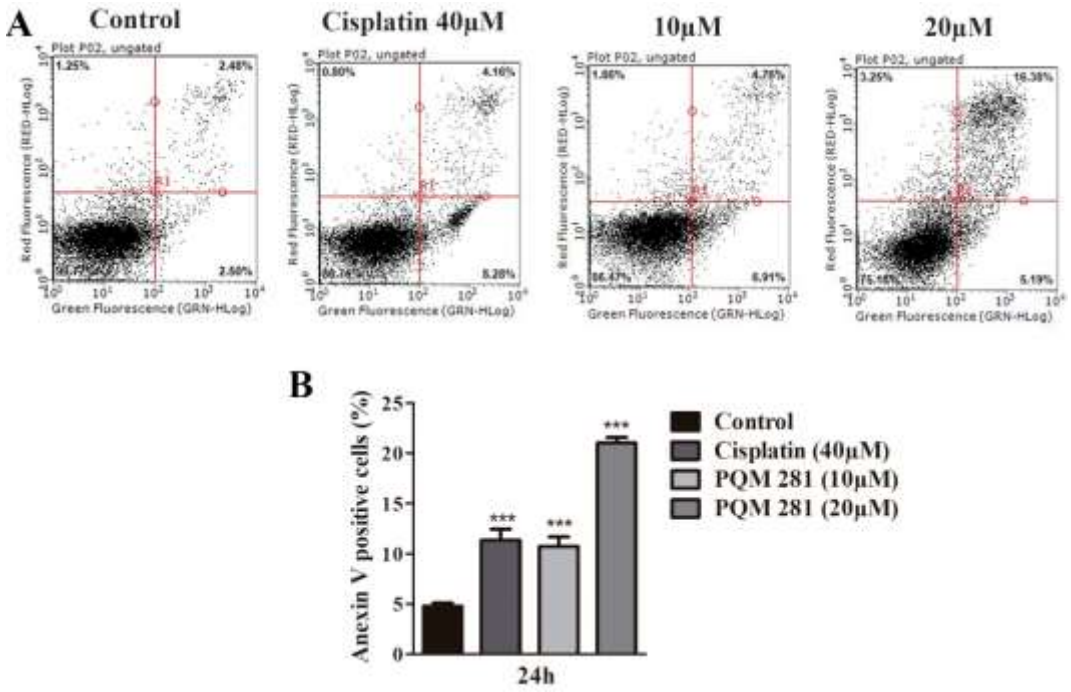

Source: From the author

Note: (A and B) Representative dot plots and analysis from annexin V/ propidium iodide (PI) assays performed in SK-MEL-147 cultures after 24 h after treatment with PQM 281 at 10 or 20 µM. Viable cells (lower left quadrants), early apoptosis (lower right quadrants), late apoptosis (upper right quadrants), and necrotic cells (upper left quadrants). Cisplatin at 40 µM was used as positive control.*** $p<0.001$ according to ANOVA followed by Dunnet post-test.

Figure 15- Annexin V/ propidium iodide (PI) assays.

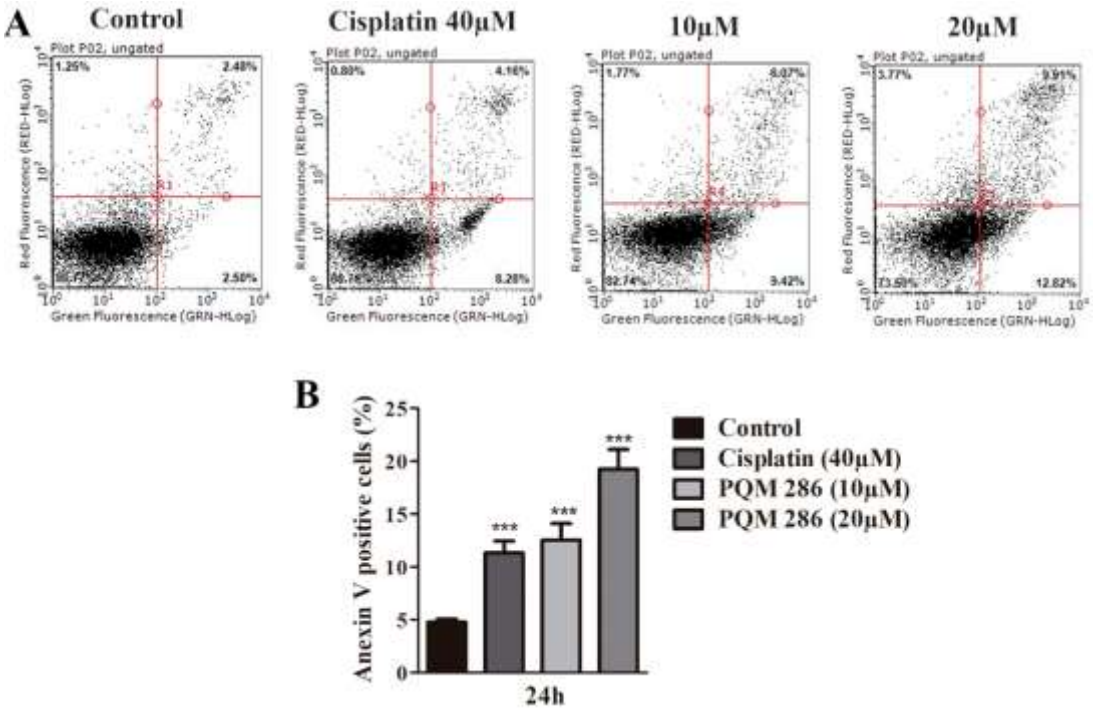

Source: From the author

Note: (A and B) Representative dot plots and analysis from annexin V/ propidium iodide (PI) assays performed in SK-MEL-147 cultures after 24 h after treatment with PQM 286 at 10 or 20 µM. Viable cells (lower left quadrants), early apoptosis (lower right quadrants), late apoptosis (upper right quadrants), and necrotic cells (upper left quadrants). Cisplatin at 40 µM was used as positive control. *** $p<0.001$ according to ANOVA and Dunnet post-test.

6 DISCUSSION

In the present study, we evaluated antitumor potential of a series of piperine-chlorogenic acid hybrids (PQM 277 – PQM 288) on malignant melanoma cell lines SK-MEL-147, CHL-1 and WM1366. These cell lines possess distinct genetic features and are representative of different melanoma subtypes. SK-MEL-147 has mutation in *NRAS* (Q61R), that contribute for hyperactivation of MAPK signaling pathway and consequently activation of proliferative signals; WM1366 harboring mutation in *NRAS* (Q61L) and *TP53* (E258K), these genetic alterations lead to continuous activation of proliferation pathways and resistance to apoptosis induction; CHL-1 has mutation in *TP53* (H193R) and *CDKN2A* (W100stop), impairing appropriate cellular response to regulatory signals of cell cycle and apoptosis.

The hyperactivation in MAPK/RAF/MEK/ERK signaling pathway is commonly observed in malignant melanoma due to mutations in *NRAS* or *BRAF*. Mutations in these proto-oncogenes are observed in 15-30% and 50-70%, respectively (CURTIN *et al*., 2005; HELD, 2010). Mutations in *CDKN2A* and *TP53* are also observed in approximately 44% and 15% of the cases, respectively, and generally associated to protein inactivation (RAJKUMAR; WATSON, [s.d.]; ZHANG *et al*., 2016). Furthermore, other alterations have been described including overexpression of Bcl-2, NF-kB and Akt-3 and loss of PTEN (GRAY-SCHOPFER; WELLBROCK; MARAIS, 2007). These genetic alterations have a critical role for the aggressive behavior of melanoma cells and drug resistance (SOENGAS; LOWE, 2003).

The synthesized substances were screened at 25 µM on three melanoma cell lines. We observed that SK-MEL-147 cell line was more sensitive than WM1366 and CHL-1. Although PQM 281, 285, 286, 287, and 288 significantly reduced cell viability rate in SK-MEL-147 cultures, the PQM 277, PQM 281 and PQM 286 were the most active compounds. We tested these substances on normal cells (FBM, fibroblast derived from normal skin) and no cytotoxic activity was observed under tested concentration range. Based on these preliminary data, SK-MEL-147 cell line and hybrid analogs PQM-277, PQM 281 and PQM 286 were selected for further investigations.

The cytotoxic profile of PQM 277 on SK-MEL-147 was more effective than cisplatin or parent compounds (**1**) and (**2**). Regarding the samples PQM 281 and PQM 286, they presented IC_{50} values similar to cisplatin and were also more effective than compounds (**1**) and (**2**). In the present study, dose-response curves were obtained using 0-100 µM concentration range. In this experimental condition, neither (**1**) nor (**2**) were able to reduce cell viability in SK-MEL-147 cultures. These data seem to be coherent once IC_{50} values determined for (**1**) on

hepatocellular carcinoma (HepG2), triple-negative breast cancer (MDA-MB-231) and non-small-cell lung cancer (A549) cell lines were approximately 200 µM (DA FONSECA *et al.*, 2020). When (**1**) was assayed on melanoma cell lines A375SM (highly metastatic) and A375P (moderately metastatic), the IC_{50} values found were around 150 µM (YOO *et al.*,2019). Additionally, IC_{50} values determined for (**2**) on osteosarcoma (U2OS, Saos-2, MG-63) cell lines were approximately 100 µM (SAPIO *et al.*, 2019).

We further demonstrated that PQM 277 at 5 or 10 µM and PQM 281 and PQM 286 at 10 or 20 µM effectively inhibit clonogenic capacity of SK-MEL-147 cells. These findings demonstrate a prolonged inhibitory effect of these substances on proliferative behavior of SK-MEL-147 cells. It has been reported that (**2**) inhibits clonogenic capacity of human osteosarcoma cell lines (U2OS, MG-63) at concentration around 100 µM (SAPIO *et al.*, 2020). Another study reported that (**1**) at 80 µM was effective to inhibit clonogenic capacity of HeLa cells (HAN *et al.*, 2017). Our results showed that PQM 277, 281 and 286 were effective to reduce clonogenic capacity of SK-MEL-147 at low concentrations.

Further we demonstrated that PQM 277 inhibits cell cycle progression at G2/M in SK-MEL-147 once cell cycle analysis showed increased G2/M population and mitotic index evidenced a accumulate of the cells in prometaphase and metaphase. Already, PQM 281 and 286 inhibited cell cycle at G1/S transition as demonstrated by increasing of the G1 population with a concomitant reduction in the frequency of cells in the S-phase.

PQM 277 there is a hydroxyl group in the para (1,4) position and a methoxyl group in the meta (1,3) position, while PQM 286 presents an ortho-substituted hydroxyl group (1,2) and a methoxyl group in the meta (1,3) position, making PQM 277 and PQM 286 positional isomers. On the other hand, PQM 281 has no substituents on the aromatic ring. Thus, structural differences of PQM 277 and PQM 286 seems to be critical for their effects on cell cycle progression. However, we can also observe that biological effect of PQM 281 was similar to observed for PQM 286, indicating that the absence of substituents on the aromatic ring seems does not significantly change its activity on proliferative behavior of SK-MEL-147.

Based on these results, molecular mechanism associated to antiproliferative activity of PQM 277, PQM 281, and PQM 286 on SK-MEL-147 was investigated. Thus, we assessed expression profiles of critical regulators of G1/S and G2/M transitions (LAPENNA; GIORDANO, 2009; MATTHEWS; BERTOLI; BUIN, 2022; OTTO; SICINSKI, 2017).

PQM 277 induced *CCNB1* and *CDK1* downregulation in SK-MEL-147 cells. Reduction of cyclin B at protein levels was also observed in response to this compound, mainly at 5 µM,

indicating that the signaling necessary for entry to mitosis was disrupted by treatment. The cyclin B-cyclin-dependent kinase 1 (CDK1) complexes are critical to promote G2/M transition and supply mitosis progression (JOUKOV; NICOLO, 2018; MATTHEWS; BERTOLI; BUIN, 2021; LAPENNA; GIORDANO, 2009; ABBAS; DUTTA, 2009; LAPENNA; GIORDANO, 2009; MATTHEWS; BERTOLI; BUIN, 2021). In parallel, we evidenced expressive increase in *CDKN1A* mRNA levels in samples treated with PQM 277 compared to control groups. *CDKN1A* encodes p21 (a member of the Kip/Cip family), an inhibitor of the different cyclin-CDK complexes (ABUKHDEIR; PARK, 2008; KREIS; LOUWEN; YUAN, 2019; LAPENNA; GIORDANO, 2009). However, it has been reported that p21 may act as tumor promoter or tumor suppressor depending on its cellular localization and cellular context. The cytoplasmic concentration of p21 favors cell growth and survival, however, nuclear localization can result in cell cycle arrest by different stressors signals (GEORGAKILAS; MARTIN; BONNER, 2017). Importantly, our results showed a significant augment in the frequency of positive cells for p21, which localization was exclusively nuclear. Increased p21 levels has been observed in response to checkpoint activation at G1/S or G2/M transition by different stimuli (GILLIS *et al*., 2009; MATTHEWS; BERTOLI; BUIN, 2022).

Mitosis is controlled by reversible protein phosphorylation involving specific kinases and phosphatases (MATTHEWS; BERTOLI; BUIN, 2022).The cyclin B–CDK1 complexes, Aurora kinases, and Polo-like kinase 1 (PLK1) cooperatively regulate and phosphorylate distinct mitotic processes (JOUKOV; NICOLO, 2018; MATTHEWS; BERTOLI; BUIN, 2021). These Auroras kinases have a key role in controlling chromosome arrangements and checking proper formation of the mitotic spindle apparatus during cell division (BORISA; BHATT, 2017; LAPENNA; GIORDANO, 2009). Once we observed cells with altered pattern of microtubule network and increased frequency of cell in prophase and metaphase in SK-MEL-147 cultures treated with PQM 277, we evaluated the gene expression at mRNA levels of *Aurora A*, *Aurora B* and *PLK1*. These mitotic kinases are frequently overexpressed in cancers and are considered as attractive anticancer drug targets (BORISA; BHATT, 2017; LENS; VOEST; MEDEMA, 2010).

Aurora-A drives centrosome maturation and contribute to centrosome separation and bipolar spindle assembly (BORISA; BHATT, 2017; JOUKOV; NICOLO, 2018; LAPENNA; GIORDANO, 2009). Aberrant Aurora-A kinase activity has been implicated in oncogenic transformation through the development of chromosomal instability and tumor cell heterogeneity, and overexpression or gene amplification of Aurora kinases has been clarified

in a number of cancers including melanoma (PUIG-BUTILLE *et al*., 2017; PUNT *et al*., 2021; WANG; MOSCHOS; BECKER, 2010; ZDIORUK *et al*., 2020), and Aurora overexpression has been correlated with poor survival rate in melanoma patients (PUIG-BUTILLE *et al*., 2017). It has been demonstrated that inhibition of Aurora kinases could potentiate the effect of chemotherapeutic agents (AMIN *et al*., 2017). Importantly, recent studies revealed a novel non-mitotic role of Aurora-A activity in promoting tumor progression through activation of epithelial–mesenchymal transition reprograming resulting in the genesis of tumor-initiating cells (D'ASSORO; HADDAD; GALANIS, 2016; DU *et al*., 2021).

Aurora-B is known as chromosomal passenger protein and localizes at the chromosome arms and at centromeres during prophase. Afterward, Aurora-B moves towards the inner centromere region followed by the central spindle and cortex during anaphase and finally accumulates in the midbody in telophase (BASANT *et al*., 2015; JOUKOV; NICOLO, 2018). Overexpression of Aurora B in cancer cells has been widely reported (BONET *et al*., 2012). A recent study demonstrated that drug-resistant melanoma cell lines display higher Aurora B expression compared to their parental cell lines. The Aurora B inhibition triggers cell cycle arrest, cellular senescence, and cell death by mitotic catastrophe or apoptosis in melanoma cells (BONET *et al*., 2012; WANG; MOSCHOS; BECKER, 2010; ZDIORUK *et al*., 2020).

PLK1 is a serine–threonine protein kinase involved in activation of CDK1–cyclin B at the G2 to M phase transition, centrosome maturation, spindle formation, chromosome segregation and cytokinesis (JOUKOV; NICOLO, 2018; LAPENNA; GIORDANO, 2009; NIGG, 2001). It was reported that mutant NRAS induces PLK1 expression, and pharmacologic inhibition of PLK1 stabilizes the size of NRAS mutant melanoma xenografts (POSCH *et al*., 2015). Recent study showed that combined inhibition of PLK1 and NOTCH significantly reduced cell proliferation of A375 and SK-MEL-2 melanoma cells (SU *et al*., 2021)

In the present study we showed that PQM-277 disturbed of the microtubule network and significantly modulated expression profiles of mitotic kinases. The abundance of mRNA for Auroras A/B and PKL1 was significantly reduced in treated samples compared to control groups. These finding are very promising and reinforce antitumor potential of PQM-277. Antimitotic agents are widely used in cancer therapy by disturbing tubulin polymerization and bipolar spindle assembly. These events lead to mitotic checkpoint activation and mitosis arrest that, ultimately, may induce cell death (JORDAN; WILSON, 2004; LAPENNA; GIORDANO, 2009). Additionally, substances with inhibitory effect on mitotic kinases, which are required

for mitosis progression, are valuable as anticancer agents (LAPENNA; GIORDANO, 2009; SINHA; DUIJF; KUM, 2019).

The analysis of the expression profiles of regulatory proteins of G1/S transition (LAPENNA; GIORDANO, 2009; MATTHEWS; BERTOLI; BUIN, 2022) revealed that PQM 281 was able to reduce cyclins D and E, which are required to activate CDK4/6 and CDK2 respectively. Thus, the data indicate that inhibitory effect of PQM 286 on proliferation of SK-MEL-147 is associated to G1/S cyclins downregulation. However, expression profiles of these cyclins are not altered by PQM 286 treatment. Considering that gene expression for cell cycle progression and survival may be regulated by mitogen-activated protein kinase (MAPK) and the phosphoinositol-3-kinase (PI3K)/AKT signaling pathways (CHAPPELL *et al*., 2011; HODIS *et al*., 2012; LEONARDI *et al*., 2018; RAHMATI *et al*., 2020; SCHADENDORF *et al*., 2015), we evaluated expression. of p-ERK and p-AKT in samples treated with PQM-277, PQM-281, and PQM 286.

We observed a slight reduction of p-ERK and p-AKT in samples treated with PQM 277 at 5 µM compared to control groups, however the differences were not statically significant. The data indicate that SK-MEL-147 proliferation inhibition promoted by PQM 277 does not seem directly to involve modulation of MAPK/ERK or PI3K/ AKT signaling pathways. We hypothesized that antiproliferative activity of PQM 277 is preferentially associated with activation of p21 activation in response to cellular stress caused by mitotic apparatus disturb (KREIS; LOUWEN; YUAN, 2019; TRAKALA *et al*., 2013; TSUDA *et al*., 2017). Regarding PQM 281 and PQM 286, our results showed that these substances induce ERK phosphorylation. Although the p-ERK levels has been slightly increased in samples treated with PQM 286, the difference was statistically significant. Already in relation to ability to modulate PI3K/AKT signaling, we found that PQM 286 significantly reduced levels of p-AKT thereby reducing survival signals, while PQM 281 has no action on this signaling pathway.

Studies show that MEK/ERK activation may induce apoptosis by both intrinsic and extrinsic pathway (CAGNOLAND; CHAMBARD, 2009; BASTOLA *et al*., 2017). Therefore, we investigated the pro-apoptotic activity of PQM 277, PQM 281 and PQM 286 on SK-MEL-147 cells. It well documented that stress caused by cell cycle arrest could lead to apoptosis (ORTH *et al*., 2012). The data showed that the three compounds are able to induce apoptosis in SK-MEL-147 cells. Increased frequency of cells positive for annexin V was observed in all treated groups when compared to controls. Further, we demonstrated that PQM 277 was able to activate intrinsic apoptotic pathway in SK-MEL-147 cells due to its capacity to modulate

Bax and *Bcl-2* expression leading to increase of the *Bax/Bcl-2* ratio. The balance between pro-apoptotic and pro-survival Bcl-2 family proteins is critical to determine whether a cell will die or live (SINGH; LETAI; SAROSIEK, 2019). The intrinsic pathway involves cytotoxic stimuli and proapoptotic signal-transducing molecules that converge on mitochondria to induce outer mitochondrial membrane permeabilization by BCL2 family of proteins, mitochondrial lipids, proteins that regulate bioenergetic metabolite flux and components of the permeability transition pore (FULDA; DEBATIN, 2006; GALLUZZI; VITALE, 2018; SINGH; LETAI; SAROSIEK, 2019). Importantly, pro-survival members of Bcl-2 family including Bcl-2 and Bcl-X_L are overexpressed in melanoma cells, which are associated with melanoma progression and resistance to therapy (EBERLE; HOSSINI, 2008; TRISCIUOGLIO; BUFALO, 2021). Our study demonstrated that PQM 277 at low concentrations induced apoptosis in SK-MEL-147 melanoma cell line by modulating *BAX* and *Bcl-2* expression leading to activation of intrinsic apoptosis pathway.

Pro-apoptotic activity of (**1**) has been reported on breast cancer (MCF-7 and MDA-MB-231) and melanoma (A375SM and A375P) cell lines, however this event was observed only when high concentrations were used (50-150 µM) (CHEN *et al*., 2020; YOO *et al.*, 2019). Likewise, (**2**) at 40 µM induced increase of the Bax/Bcl-2 ratio leading to activation of intrinsic apoptosis pathway on human kidney cancer cell line (A498) (WANG *et al.*, 2019).

Lastly, we sought to evaluate whether cell cycle arrest and apoptosis induced by PQM 277 could be associated to DNA damage. It is known that to maintenance of genomic integrity after DNA damage depends on the coordinated action of the DNA repair system and cell cycle checkpoint controls (HIRAO *et al*., 2000). Cell cycle arrest in G1, S or G2 phase is maintained until DNA integrity is restored. However, if lesions are irreparable, programmed cell death is induced by the ATM–ATR signaling pathway (SHILOH, 2003). DNA damage is sensed by several specialized proteins and triggers cell cycle arrest via checkpoint kinase 2 (CHK2) or via checkpoint kinase 1 (CHK1). The ATM-CHK2 pathway regulates the G1 checkpoint, whereas the ATR-CHK1 pathway regulates the S and G2 checkpoints, although there is crosstalk between these pathways (LAPENNA; GIORDANO, 2009; MENOLFI; ZHA, 2020; OTTO; SICINSKI, 2017; SHAPIRO, 2006; SHILOH, 2003). Thus, comet assay was performed to evaluate the ability of PQM 277 to induce DNA damage, however the data showed that there was no DNA fragmentation in the evaluate experimental conditions. However, it is possible that DNA damage may be occurred and we could not detect it. In parallel, we investigated the *CHK*2 gene expression, but the mRNA abundance for this gene was reduced in samples treated

with PQM 277. Taken together, the data showed that PQM-277-induced apoptosis was not involved with DNA fragmentation and activation of ATM- CHK2 pathway.

Oxidative stress also can activate intrinsic apoptotic pathway. Thus, we investigated a possible modulation in Nuclear 2-related erythroid factor 2 (NRF2) expression as a consequence of PQM 277 treatment. NFR2 is a master regulator of antioxidant response, maintaining redox homeostasis in the cells. Under physiological conditions NRF2 binds to KEAP1 (Kelchlike ECH associated protein 1), which directs NRF2 continuously to proteosome degradation (RIBEIRO *et al*., 2016; SAJADIMAJD; KHAZAEI, 2018). However, in oxidative stress situations, KEAP1 is oxidized and NRF2 is translocated into the nucleus where it can activate and regulates the expression of multiple antioxidant genes, thereby neutralizing the reactive oxygen species to restore cellular redox balance (SAJADIMAJD; KHAZAEI, 2018; SPORN; LIBY, 2012; XUE; ZHOU; QIU, 2020). We did not observe significant difference in mRNA abundance for *NRF2* to compare results from treated and control groups. Thus, pro-apoptotic activity of PQM 277 is not associated to DNA damage or oxidative stress.

7 CONCLUSION

In the present study, we tested a series of piperine-chlorogenic hybrids regarding their antitumor potential. The substances were screened on melanoma cell lines with different genetic features. SK-MEL-147 cells were more sensitive to treatments than CHL-1 or WM-1366. PMQ-277, PQM 281 and PQM 286 showed to be the most active substance compared to other synthesized hybrids analogs. Notably, the lead compounds were more active than to their parental compounds (alone or in combination). The mechanistic study showed that PQM 277 inhibits proliferation by modulation mitotic kinases that, in turn, lead to mitotic arrest and apoptosis. PQM 281 inhibits proliferative behavior of SK-MEL-147 cell by promoting cyclins D and E downregulation and induces apoptosis via ERK activation. PQM 286 seems act preferentially as a cytotoxic agent by reducing PI3K/AKT signaling pathway. Our findings demonstrated that these three compounds are promising anticancer drug candidates and support further *in vivo* investigations.

REFERENCES

ABBAS, T.; DUTTA, A. p21 in cancer : intricate networks and multiple activities. **Nature Reviews Cancer**, Virginia, v. 9, n. 6, p. 400–414, 2009.

ABUKHDEIR, A. M.; PARK, B. H. p21 and p27 : roles in carcinogenesis and drug resistance. **Expert Reviews in Molecular Medicine**, Cambridge, v. 10, p. e19, 2008.

AKBANI, R. *et al*. Genomic classification of cutaneous. **Cell**, [s. l.], v. 161, n. 7, p. 1681–1696, 2015.

AMIN, M. *et al*. A phase I study of MK-5108, an oral aurora A kinase inhibitor, administered both as monotherapy and in combination with docetaxel, in patients with advanced or refractory solid tumors. **Investigational New Drugs**, New York, v. 34, n. 1, p. 84–95, 2017.

ASATI, V.; MAHAPATRA, D. K.; BHARTI, S. K. European Journal of Medicinal Chemistry PI3K / Akt / mTOR and Ras / Raf / MEK / ERK signaling pathways inhibitors as anticancer agents : Structural and pharmacological perspectives. **European Journal of Medicinal Chemistry**, [s. l.], v. 109, p. 314–341, 2016.

ASCIERTO, P. A. *et al*. Cobimetinib combined with vemurafenib in advanced BRAF V600 - mutant melanoma (coBRIM): updated effi cacy results from a randomised , double-blind , phase 3 trial. **Lancet Oncology**, [s. l.], v. 17, n. 9, p. 1248–60, 2016.

AZEVEDO-BARBOSA, H. *et al*. Phenylpropanoid-based sulfonamide promotes cyclin D1 and cyclin E down-regulation and induces cell cycle arrest at G1/S transition in estrogen positive MCF-7 cell line. **Toxicology in Vitro**, [s. l.], v. 59, n. 1, p. 150–160, 2019.

BAGDAS, D. *et al*. Pharmacologic overview of systemic chlorogenic acid therapy on experimental wound healing. **Naunyn-Schmiedeberg's Arch Pharmacol**, [s. l.], v. 387, p. 1101–1116, 2014.

BAGDAS, D.; CINKILIC, N.; YUCEL, H. Antihyperalgesic activity of chlorogenic acid in experimental neuropathic pain. **Journal of Natural Medicines**, [s. l.], v. 67, n. 4, p. 698–704, 2012.

BASANT, A. *et al*. Aurora B Kinase promotes cytokinesis by inducing centralspindlin oligomers that associate with the article Aurora B kinase promotes cytokinesis by inducing centralspindlin oligomers that associate with the plasma membrane. **Developmental Cell**, [s. l.], v. 33, n. 2, p. 204–215, 2015.

BERTOLI, G.; CAVA, C.; CASTIGLIONI, I. Micrornas: new biomarkers for diagnosis, prognosis, therapy prediction and therapeutic tools for breast cancer. **Theranostics**, [s. l.], v. 5, n. 10, p. 1122–1143, 2015.

BONESI, M. *et al*. Exploring the anti-proliferative , pro-apoptotic , and antioxidant properties of. **Biomedicine & Pharmacotherapy journal**, [s. l.], v. 107, p. 967–978, 2018.

BONET, C. *et al*. Aurora B is regulated by the mitogen-activated protein kinase / extracellular signal-regulated kinase (MAPK / ERK) signaling pathway and is a valuable potential target in melanoma cells *. **Journal of Biological Chemistry**, [s. l.], v. 287, n. 35, p. 29887–29898, 2012.

BORISA, A. C.; BHATT, H. G. European Journal of Medicinal Chemistry Review article A comprehensive review on Aurora kinase : Small molecule inhibitors and clinical trial studies. **European Journal of Medicinal Chemistry**, [s. l.], v. 140, p. 1–19, 2017.

BRAY, F.; FERLAY, J.; SOERJOMATARAM, I. Global cancer statistics 2018 : GLOBOCAN estimates of incidence and mortality worldwide for 36 cancers in 185 countries. **Cancer Journal for Clinicians**, [s. l.], v. 68, p. 394–424, 2018.

CARLINO, M. S. *et al*. Targeting oncogenic BRAF and aberrant MAPK activation in the treatment of cutaneous melanoma. **Critical Reviews in Oncology/Hematology**, Ireland, v. 96, n. 3, p. 385–398, 2015.

CHAFFER, C. L.; WEINBERG, R. A. A perspective on cancer cell metastasis. **Science**, [s. l.], v. 331, n. 6024, p. 1559–1565, 2011.

CHANG, C.; CHANG, Y.; TSENG, T. Mulberry leaf extract inhibit hepatocellular carcinoma cell proliferation via depressing IL-6 and TNF- a derived from adipocyte. **Journal of Food and Drug Analysis**, [s. l.], n. 110, p. 1–9, 2018.

CHAPPELL, W. H. *et al*. Ras/Raf/MEK/ERK and PI3K/PTEN/Akt/mTOR inhibitors: rationale and importance to inhibiting these pathways in human health. **Oncotarget**, [s. l.], v. 2, n. 3, p. 135–164, 2011.

CHEN, D. *et al*. Two natural alkaloids synergistically induce apoptosis in breast cancer cells by inhibiting STAT3 activation. **Molecules**, [s. l.], v. 25, n. 1, p. 216, 2020.

CINKILIC, N. *et al*. Radioprotection by two phenolic compounds : Chlorogenic and quinic acid , on X-ray induced DNA damage in human blood lymphocytes in vitro. **Food and Chemical Toxicology Journal**, [s. l.], v. 53, p. 359–363, 2013.

CLARK, W. H. Tumour progression and the nature of cancer *. **British Journal of Cancer - Nature**, Pennsylvannia, v. 64, n. 3, p. 631–644, 1991.

CURTIN, J. A. *et al*. Distinct sets of genetic alterations in melanoma. **The New England Journal of Medicine Original**, Massachusetts, v. 353, n. 20, p. 2135–2147, 2005.

D'ASSORO, A. B.; HADDAD, T.; GALANIS, E. Aurora-A Kinase as a promising therapeutic target in cancer. **Frontiers in Oncology**, [s. l.], v. 5, p. 1–8, 2016.

DA FONSECA, L. M. *et al*. Piperine inhibits TGF- β signaling pathways and isrupts EMT-related events in human lung. **Medicines**, [s. l.], v. 7, n. 19, p. 1–16, 2020.

DAVIES, M. A. The role of the PI3K-AKT pathway in melanoma. **Cancer Journal**, Houston, v. 18, n. 2, p. 142–147, 2012.

DESSINIOTI, C. *et al*. Melanocortin 1 receptor variants : functional role and pigmentary associations. **Photochemistry and Photobiology**, [s. l.], v. 87, n. 18, p. 978–987, 2011.

DING, Y. *et al*. Development and evaluation of a novel drug delivery: soluplus®/TPGS mixed micelle loaded with piperine in vitro and in vivo. **Drug Development and Industrial Pharmacy,** [s. l.], v. 44, n. 9, p. 1409–1416, 2018.

DOBRY, A. S. *et al*. Management of metastatic melanoma : improved survival in a national cohort following the approvals of checkpoint blockade immunotherapies and targeted therapies American Joint Committee on Cancer. **Cancer Immunology, Immunotherapy**, [s. l.], v. 67, p. 1833–1844, 2018.

DOUCETTE, C. D. *et al*. Piperine , a dietary phytochemical , inhibits angiogenesis. **Journal of Nutritional Biochemistry**, [s. l.], v. 24, p. 231–239, 2013.

DRÃGÃNESCU, M.; CARMOCAN, C. Hormone therapy in breast cancer. **Chirurgia**, [s. l.], v. 112, n. 4, p. 413–417, 2017.

DU, R. *et al*. Targeting AURKA in cancer : molecular mechanisms and opportunities for cancer therapy. **Molecular Cancer**, [s. l.], v. 20, n. 1, p. 1–27, 2021.

DUMMER, R. *et al*. Encorafenib plus binimetinib versus vemurafenib or encorafenib in patients with BRAF -mutant melanoma (COLUMBUS): a multicentre , open-label , randomised phase 3 trial. **Lancet Oncology**, [s. l.], v. 19, n. 5, p. 603–615, 2018.

EDDY, K.; CHEN, S. Overcoming immune evasion in melanoma. **International Journal of Molecular Sciences**, [s. l.], v. 21, n. 23, p. 12–16, 2020.

EGGERMONT, A. M. M. *et al*. Cutaneous melanoma. **Lancet**, [s. l.], v. 383, n. 9919, p. 816–27, 2014.

EKBATAN, S. S. *et al*. Chlorogenic acid and its microbial metabolites exert anti-proliferative effects , S-phase cell-cycle arrest and apoptosis in human colon cancer Caco-2 cells. **Molecular Sciences Article**, [s. l.], v. 19, p. 723, 2018.

EMRI, G.; JANKA, E.; JANKA, E. Ultraviolet radiation-mediated development of cutaneous melanoma: An update. **Journal of Photochemistry and Photobiology B**, [s. l.], v. 185, p. 169–175, 2018.

FERREIRA-SILVA, G. A. *et al*. [Ru(pipe)(dppb)(bipy)]PF6: A novel ruthenium complex that effectively inhibits ERK activation and cyclin D1 expression in A549 cells. **Toxicology In Vitro**, [s. l.], v. 44, p. 382–391, 2017.

FOFARIA, N. M.; KIM, S.; SRIVASTAVA, S. K. Piperine causes G1 phase cell cycle arrest and apoptosis in melanoma cells through checkpoint kinase-1 activation. **Plos One**, Italy, v. 9, n. 5, p. 1–10, 2014.

FRANKEN, N. A. P. *et al*. Clonogenic assay of cells in vitro. **Nature Protocols**, [s. l.], v. 1, n. 5, p. 2315–2319, 2006.

FULDA, S.; DEBATIN, K. Extrinsic versus intrinsic apoptosis pathways in anticancer chemotherapy. **Oncogene**, [s. l.], v. 25, n. 34, p. 4798–4811, 2006.

GALLUZZI, L.; VITALE, I. Molecular mechanisms of cell death : recommendations of the nomenclature committee on cell eath 2018. **Cell Death & Differentiation**, [s. l.],v. 25, n. 3, p. 486–541, 2018.

GEORGAKILAS, A. G.; MARTIN, O. A.; BONNER, W. M. p21 : A two-faced genome guardian. **Trends in Molecular Medicine: Cell Press**, [s. l.], v. 23, n. 4, p. 310–319, 2017.

GEORGE, K.; SUSAN, N.; MALATHI, R. Piperine blocks voltage gated K + current and inhibits proliferation in androgen sensitive and insensitive human prostate cancer cell lines. **Archives of Biochemistry and Biophysics**, [s. l.], v. 667, p. 36–48, 2019.

GILLIS, L. D. et al. p21Cip1/WAF1 mediates cyclin B1 degradation in response to DNA damage. **Cell Cycle**, [s. l.], v. 8, n. 2, p. 253–6, 2009.

GORGANI, L. *et al.* Piperine — the bioactive compound of black pepper : from isolation to medicinal formulations. **Comprehensive Reviews in Food Science and Food Safety**, [s. l.], v. 16, n. 1, p. 1–17, 2017.

GRAY-SCHOPFER, V.; WELLBROCK, C.; MARAIS, R. Melanoma biology and new targeted therapy. **Nature**, [s. l.], v. 445, n. 7130, p. 851–7, 2007.

GROSSMAN, D. *et al*. Prognostic gene expression profiling in cutaneous melanoma identifying the knowledge gaps and assessing the clinical benefit. **JAMA Dermatology**, [s. l.], v. 156, n. 9, p. 1004–1011, 2020.

GUARNERI, C. *et al.* NF - κ B inhibition is associated with OPN / MMP - 9 downregulation in cutaneous melanoma. **Oncology Reports**, [s. l.], v. 37, n. 2, p. 737–746, 2017.

GUO, Z. *et al*. Anti-inflammatory and antitumour activity of various extracts and compounds from the fruits of Piper longum L. **Journal of Pharmacy and Pharmacology**, [s. l.], v. 71, p. 1162–1171, 2019.

HAN, S. *et al*. Piperine (PP) enhanced mitomycin-C (MMC) therapy of human cervical cancer through suppressing Bcl-2 signaling pathway via inactivating STAT3 / NF- κ B. **Biomedicine & Pharmacotherapy**, [s. l.], v. 96, p. 1403–1410, 2017.

HANAHAN, D.; WEINBERG, R. A. Review hallmarks of cancer : the next generation. **Cell**, [s. l.], v. 144, n. 5, p. 646–674, 2011.

HANAHAN, D.; WEINBERG, R. A.; FRANCISCO, S. The hallmarks of cancer review university of california at san francisco. **Cell**, [s. l.], v. 100, n. 1, p. 57–70, 2000.

HAWKES, J. E.; TRUONG, A.; LAURENCE, J. Genetic predisposition to melanoma. **Seminars Oncology**, Salt Lake City, v. 43, n. 5, p. 591–597, 2016.

HELD, M. A. Genetic alterations in malignant melanoma. **Diagnostic Histopathology**, [s. l.], v. 16, n. 7, p. 317–320, 2010.

HERLYN, M. Human melanoma: development and progression. **Cancer and Metastasis Reviews**, [s. l.], v. 9, n. 2, p. 101–112, 1990.

HIRAO, A. *et al*. DNA damage-induced activation of p53 by the checkpoint kinase ChkZ. **Science**, [s. l.], v. 287, n. 5459, p. 1824–1827, 2000.

HODI, F. *et al*. Improved survival with ipilimumab in patients with metastatic melanoma. **The New England Journal of Medicine**, Massachusetts, v. 363, n. 8, p. 711–723, 2010.

HODI, F. S. *et al*. Combined nivolumab and ipilimumab versus ipilimumab alone in patients with advanced melanoma : 2-year overall survival outcomes in a multicentre , randomised , controlled , phase 2 trial. **Lancet Oncology**, [s. l.], v. 17, n. 11, p. 1558–1568, 2016.

HODIS, E. *et al*. A Landscape of driver mutations in a landscape of driver mutations in melanoma. **Cell**, [s. l.], v. 150, n. 2, p. 251–263, 2012.

HUANG, S. *et al*. Theranostics chlorogenic acid effectively treats cancers through induction of cancer cell differentiation. **Theranostics**, [s. l.], v. 9, n. 23, p. 6745–6763, 2019.

ISOLA, A. L.; EDDY, K.; CHEN, S. Biology , therapy and implications of tumor exosomes in the progression of melanoma. **Cancers (Basel)**, [s. l.], v. 8, n. 12, p. 110, 2016.

JAFRI, A. *et al.* Induction of apoptosis by piperine in human cervical adenocarcinoma via ros mediated mitochondrial pathway and caspase-3 activation. **Excli Journal**, [s. l.], v. 18, p. 154–164, 2019.

JAKOB, J. A. *et al*. NRAS mutation status is an independent prognostic factor in metastatic melanoma. **Cancer**, [s. l.], v. 118, n. 16, p. 4014–4023, 2012.

JIANG, B. *et al*. Poly (N -phenylglycine) -based nanoparticles as highly effective and targeted near-infrared photothermal therapy / photodynamic therapeutic agents for malignant melanoma. **Small**, [s. l.], v. 13, n. 8, p. 1–15, 2017.

JORDAN, M. A.; WILSON, L. Microtubules as a target for anticancer drugs. **Nature Reviews Cancer**, [s. l.], v. 4, p. 253–265, 2004.

JOUKOV, V.; NICOLO, A. DE. Aurora-PLK1 cascades as key signaling modules in the regulation of mitosis. **Science Signaling**, [s. l.], v. 11, n. 545, p. 1–26, 2018.

KRAUTHAMMER, M. *et al.* Exome sequencing identifies recurrent mutations in NF1 and RASopathy genes in sun-exposed melanomas. **Nature genetics**, [s. l.], v. 47, n. 9, p. 996–1002, 2015.

KREIS, N. N.; LOUWEN, F.; YUAN, J. The multifaceted p21 (Cip1/Waf1/CDKN1A) in cell differentiation, migration and cancer therapy. **Cancers (Basel)**, [s. l.], v. 11, n. 9, p. :1220, 2019.

KUK, D. *et al.* Prognosis of mucosal , uveal , acral , nonacral cutaneous , and unknown primary melanoma from the time of first metastasis. **Oncologist**, [s. l.], v. 21, n. 7, p. 848–854, 2016.

LAI, L. *et al*. Piperine suppresses tumor growth and metastasis in vitro and in vivo in a 4T1 murine breast cancer model. **Acta Pharmacologica Sinica**, [s. l.], v. 33, p. 523–530, 2012.

LAMARTINE-HANEMANN, S. DA S. *et al.* A tetraprenylated benzophenone 7-epiclusianone induces cell cycle arrest at G1/S transition by modulating critical regulators of cell cycle in breast cancer cell lines. **Toxicology in Vitro**, [s. l.], v. 68, p. 104927, 2020.

LAPENNA, S.; GIORDANO, A. Cell cycle kinases as therapeutic targets for cancer. **Nature Reviews Drug Discovery**, [s. l.], v. 8, n. 7, p. 547–66, 2009.

LEITER, U.; GARBE, C. Epidemiology of melanoma and nonmelanoma skin cancer— the role of sunlight. **Advances in Experimental Medicine and Biology**, [s. l.], v. 624, p. 89–103, 2008.

LENS, S. M. A.; VOEST, E. E.; MEDEMA, R. H. Shared and separate functions of in cancer. **Nature Reviews Cancer**, [s. l.], v. 10, n. 12, p. 825–41, 2010.

LEONARDI, G. C. *et al*. Cutaneous melanoma : from pathogenesis to therapy (Review). **International Journal of Oncology**, [s. l.], v. 52, n. 4, p. 1071–1080, 2018.

LIMA, L. M.; BARREIRO, E. J. Bioisosterism : a useful strategy for molecular modification and drug design. **Current Medicinal Chemistry**, [s. l.], v. 12, n. 1, p. 23–49, 2005.

LIU, J. *et al.* Exploring the antioxidant effects and periodic regulation of cancer cells by polyphenols produced by the fermentation of grape skin by lactobacillus plantarum KFY02. **Biomolecules**, [s. l.], v. 9, p. 575, 2019.

LONG, G. V. *et al.* Combined BRAF and MEK Inhibition versus BRAF inhibition alone in melanoma. **New England Journal of Medicine**, Massachusetts, v. 371, p. 1877–1888, 2014.

MADAK-ERDOGAN, Z. *et al*. Genomic collaboration of estrogen receptor and extracellular signal-regulated kinase 2 in regulating gene and proliferation programs. **Molecular and Cellular Biology**, [s. l.], v. 31, n. 1, p. 226–236, 2011.

MAERTENS, O. *et al*. Elucidating distinct roles for NF1 in melanomagenesis. **Cancer Discovery**, Massachusetts, v. 3, n. 3, p. 338–349, 2013.

MATTHEWS, H. K.; BERTOLI, C.; BUIN, R. Cell cycle control in cancer. **Nature Reviews Molecular Cell Biology**, [s. l.], v. 23, n. 1, p. 74–88, 2022.

MENOLFI, D.; ZHA, S. ATM , ATR and DNA - PKcs kinases — the lessons from the mouse models : inhibition ≠ deletion. **Cell & Bioscience**, [s. l.], v. 8, p. 1–15, 2020.

MILLET, A.; MARTIN, A. R.; RONCO, C. Metastatic melanoma : insightsiInto the evolution of the treatments and future challenges. **Medicinal Research Reviews**, [s. l.], v. 37, n. 1, p. 98–148, 2017.

NEWMAN, D. J.; CRAGG, G. M. Natural products as sources of new drugs from 1981 to 2014. **Journal of Natural Products**, [s. l.], v. 79, p. 629–661, 2016.
NIGG, E. A. Mitotic kinases as regulators of cell division and its checkpoints. **Nature Reviews Molecular Cell Biology**, [s. l.], v. 2, n. 1, p. 21–32, 2001.

NISSAN, M. H. *et al*. Loss of NF1 in cutaneous melanoma is associated with RAS activation and MEK dependence. **Cancer Research**, [s. l.], v. 74, n. 8, p. 2340–2350, 2014.

OBOH, G.; AGUNLOYE, O. M.; ADEFEGHA, S. A. Comparative study on the inhibitory effect of caffeic and chlorogenic acids on key enzymes linked to alzheimer ' s disease and some pro-oxidant induced oxidative stress in rats '. **Neurochemical Research**, [s. l.], v. 38, p. 413–419, 2013.

OLBRYT, M. *et al.* Genetic profiling of advanced melanoma : candidate mutations for predicting sensitivity and resistance to targeted therapy. **Targeted Oncology**, [s. l.], v. 15, n. 1, p. 101-113, 2020.

ORTH, J. D. *et al*. Prolonged mitotic arrest triggers partial activation of apoptosis , resulting in DNA damage and p53 induction. **Molecular Biology of the Cell**, Massachusetts, v. 23, n. 4, p. 567–576, 2012.

OTTO, T.; SICINSKI, P. Cell cycle proteins as promising targets in cancer therapy. **Nature Reviews Cancer**, [s. l.], v. 12, n. 2, p. 93–115, 2017.

OUYANG, D. *et al*. Piperine inhibits the proliferation of human prostate cancer cells via induction of cell cycle arrest and autophagy. **Food and Chemical Toxicology Journal**, [s. l.], v. 60, p. 424–430, 2013.

PAPPALARDO, F. *et al*. Computational modeling of PI3K / AKT and MAPK signaling pathways in melanoma cancer. **PLoS ONE**, [s. l.], v. 11, n. 3, p. e0152104, 2016.

PETERSON, Q. P. *et al.* Procaspase-3 activation as an anti-cancer strategy: structure- activity relationship of procaspase-activating compound 1 (PAC-1) and its cellular co-localization with caspase-3. **Journal of Medicinal Chemistry**, [s. l.], v. 52, n. 18, p. 5721–5731, 2010.

POSCH, C. *et al*. Combined inhibition of MEK and Plk1 Has synergistic antitumor activity in NRAS mutant melanoma. **Journal of Investigative Dermatology**, [s. l.], v. 135, n. 10, p. 2475–2483, 2015.

PUIG-BUTILLE, J. A. *et al*. AURKA overexpression is driven by FOXM1 and MAPK/ERK Activation in melanoma cells harboring BRAF or NRAS mutations: impact on melanoma prognosis and therapy. **Journal of Investigative Dermatology**, [s. l.], v. 137, n. 6, p. 1297–1310, 2017.

PUNT, S. *et al*. Aurora kinase inhibition sensitizes melanoma cells to T - cell - mediated cytotoxicity. **Cancer Immunology, Immunotherapy**, [s. l.], v. 70, n. 4, p. 1101–1113, 2021.

RAHMATI, M. *et al*. New insights on the role of autophagy in the pathogenesis and treatment of melanoma. **Molecular Biology Reports**, [s. l.], v. 47, n. 11, p. 9021–9032, 2020.

RAJKUMAR, S.; WATSON, I. R. Molecular characterisation of cutaneous melanoma : creating a framework for targeted and immune therapies. **British Journal of Cancer**, [s. l.], v. 115, p. 145–155.

REFOLO, M. G. *et al*. Chlorogenic acid improves the regorafenib effects in human hepatocellular carcinoma cells. **International Journal of Molecular Sciences**, [s. l.], v. 19, p. 1518, 2018.

RIBEIRO, C. *et al*. NRF2 and glutathione are key resistance temozolomide in glioma and melanoma cells mediators to. **Oncotarget**, [s. l.], v. 7, n. 30, , 2016.

ROBERT, C. *et al*. Five-Year Outcomes with Dabrafenib plus Trametinib in Metastatic Melanoma. **New England Journal of Medicine**, Massachusetts, v. 381, n. 7, p. 626–636, 2019.

RUBINSTEIN, J. C. *et al*. Incidence of the V600K mutation among melanoma patients with BRAF mutations , and potential therapeutic response to the specific BRAF inhibitor PLX4032. **Journal of Translational Medicine**, [s. l.], p. 8:67, 2010.

SAJADIMAJD, S.; KHAZAEI, M. Oxidative stress and cancer: the role of Nrf2. **Current Cancer Drug Targets**, [s. l.], v. 18, n. 8, p. 538–557, 2018.

SAMYKUTTY, A. *et al.* piperine , a bioactive component of pepper spice exerts therapeutic effects on androgen dependent and androgen independent prostate cancer cells. **Plos One**, [s. l.], v. 8, n. 6, p. 1–11, 2013.

SAPIO, L. *et al*. Chlorogenic acid activates ERK1 / 2 and inhibits proliferation of osteosarcoma cells. **Journal of Cellular Physiology**, [s. l.], v. 235, p. 1–12, 2019.

SATO, Y. *et al.* In vitro and in vivo antioxidant properties of chlorogenic acid and caffeic acid. **International Journal of Pharmaceutics**, [s. l.], v. 403, p. 136–138, 2011.

SCALBERT, A. *et al*. dietary polyphenols and the prevention of diseases dietary polyphenols. **Critical Reviews in Food Science and Nutrition**, [s. l.], v. 45, p. 287–306, 2007.

SCHADENDORF, D. *et al*. Melanoma. **Nature Reviews Disease Primers**, [s. l.], v. 1, p. 15003, 2015.

SELVENDIRAN, K.; BANU, S. M.; SAKTHISEKARAN, D. Protective effect of piperine on benzo (a) pyrene-induced lung carcinogenesis in Swiss albino mice. **Clinica Chimica Acta**, [s. l.], v. 350, p. 73–78, 2004.

SHAIN, A. H. *et al.* The genetic evolution of melanoma from precursor lesions. **The New Eengl and Journal of Medicine**, Massachusetts, v. 373, n. 20, p. 1926–1936, 2015.

SHAIN, A. H.; BASTIAN, B. C. From melanocytes to melanomas. **Nature Reviews Cancer**, San Francisco, v. 16, n. 6, p. 345–58, 2016.

SHAPIRO, G. I. Cyclin-dependent kinase pathways as targets for cancer treatment. **Journal of Clinical Oncology**, Boston, v. 24, n. 11, 2006.

SHILOH, Y. ATM and related protein kinases: safeguarding genome integrity. **Nature Reviews Cancer**, [s. l.], v. 3, n. 3, p. 155–68, 2003.

SI, L. *et al*. Piperine functions as a tumor suppressor for human ovarian tumor growth via activation of JNK / p38 MAPK- mediated intrinsic apoptotic pathway Running Head : Piperine suppress ovarian tumor growth. **Bioscience Reports**, [s. l.], v. 38, n. 3, 2018.

SIEGEL, R. L.; MILLER, K. D. Cancer statistics , 2019. **Cancer Journal for Clinicians**, [s. l.], v. 69, n. 1, p. 7–34, 2019.

SIEGEL, R. L.; MILLER, K. D. Cancer statistics , 2020. **Cancer Journal for Clinicians**, [s. l.], v. 0, n. 0, p. 1–24, 2020.

SIEGEL, R. L.; MILLER, K. D. Cancer statistics , 2021. **CA: A Cancer Journal for Clinicians**, [s. l.], v. 71, n. 1, p. 7–33, 2021.

SIEGEL, R. L.; MILLER, K. D.; JEMAL, A. Cancer statistics , 2016. **Cancer Journal for Clinicians**, [s. l.], v. 66, n. 1, p. 7–30, 2016.

SINGH, B. P.; SALAMA, A. K. S. Updates in therapy for advanced melanoma. **Cancers**, [s. l.], v. 8, n. 1, p. 1–15, 2016.

SINGH, N. P. *et al*. A simple technique for quantitation damage in individual of low levels of DNA Cells. **Experimental Cell Research**, [s. l.], v. 175, p. 184–191, 1988.

SINGH, R.; LETAI, A.; SAROSIEK, K. Regulation of apoptosis in health and disease: the balancing act of BCL-2 family proteins. **Nature Reviews Molecular Cell Biology**, [s. l.], v. 20, n. 3, p. 175–193, 2019.

SINHA, D.; DUIJF, P. H. G.; KUM, K. Mitotic slippage : an old tale with a new twist. **Cell cycle**, [s. l.], v. 18, n. 1, p. 7–15, 2019.

SOENGAS, M. S.; LOWE, S. W. Apoptosis and melanoma chemoresistance. **Oncogene**, [s. l.], v. 22, n. 20, p. 3138–3151, 2003.

SPORN, M. B.; LIBY, K. T. NRF2 and cancer : the good , the bad and the importance of context. **Nature Reviews Cancer**, [s. l.], v. 12, n. 8, p. 564–571, 2012.

SUNG, H. *et al*. Global cancer statistics 2020 : GLOBOCAN estimates of incidence and mortality worldwide for 36 cancers in 185 countries. **CA: A Cancer Journal for Clinicians**, [s. l.], v. 71, n. 3, p. 209–249, 2021.

SUT, S. *et al*. Triterpene acid and phenolics from ancient apples LC-MS study and in vitro activities. **Molecules**, [s. l.], v. 24, n. 1109, p. 1–18, 2019.

TRAKALA, M. *et al*. Aurora B prevents delayed DNA replication and premature mitotic exit by repressing p21 Cip1. **Cell**, [s. l.], v. 12, n. 7, p. 1030–1041, 2013.

TSUDA, Y. *et al.* Mitotic slippage and the subsequent cell fates after inhibition of Aurora B during tubulin-binding agent – induced mitotic arrest. **Scientific Reports**, [s. l.], v. 7, p. 16762, 2017.

VICHAI, V.; KIRTIKARA, K. Sulforhodamine B colorimetric assay for cytotoxicity screening. **Nature Protocols**, [s. l.], v. 1, n. 3, p. 1112–1116, 2006.

WANG, X. *et al.* Chlorogenic acid inhibits proliferation and induces apoptosis in A498 human kidney cancer cells via inactivating PI3K / Akt / mTOR signalling pathway. **Journal of Pharmacy and Pharmacology**, [s. l.], v. 71, n. 7, p. 1100–1109, 2019.

WANG, X.; MOSCHOS, S. J.; BECKER, D. functional analysis and molecular targeting of aurora kinases A and B in advanced melanoma. **Genes & Cancer**, [s. l.], v. 1, n. 9, p. 952–963, 2010.

WENG, C.; YEN, G. Chemopreventive effects of dietary phytochemicals against cancer invasion and metastasis : phenolic acids , monophenol , polyphenol , and their derivatives. **Cancer Treatment Reviews Journal**, [s. l.], v. 38, p. 76–87, 2012.

WU, X. *et al.* Racial and ethnic variations in incidence and survival of cutaneous melanoma in the United States. **Journal of the American Academy of Dermatology**, [s. l.], v. 65, n. 5, p. S26.e1–S26.e13, 2006.

XUE, D.; ZHOU, X.; QIU, J. Emerging role of NRF2 in ROS-mediated tumor chemoresistance. **Biomedicine & Pharmacotherapy**, [s. l.], v. 131, p. 110676, 2020.

YING, X. *et al*. International immunopharmacology piperine inhibits IL- β induced expression of in fl ammatory mediators in human osteoarthritis chondrocyte. **International Immunopharmacology**, [s. l.], v. 17, p. 293–299, 2013.

YOO, E. S. *et al*. antitumor and apoptosis-inducing effects of piperine on human melanoma cells. **Anticancer Research**, [s. l.], v. 39, n. 4, p. 1883–1892, 2019.

ZDIORUK, M. *et al.* A new inhibitor of tubulin polymerization kills multiple cancer cell types and reveals p21-mediated mechanism determining cell death after mitotic catastrophe. **Cancers**, [s. l.], v. 12, n. 8, p. 1–21, 2020.

ZENG, X. *et al.* Selective Reduction in the expression of UGTs and SULTs, a novel mechanism by which piperine enhances the bioavailability of curcumin in rat. **Biopharmaceutics & Drug Disposition**, [s. l.], v. 38, n. 1, 2017.

ZHANG, T. *et al*. The genomic landscape of cutaneous melanoma. **Pigment Cell Melanoma**, [s. l.], v. 29, n. 3, p. 266–283, 2016.